



UNIVERSIDAD DE INVESTIGACIÓN DE TECNOLOGÍA EXPERIMENTAL YACHAY

Escuela de Ciencias Químicas e Ingeniería

TÍTULO: Synthesis and Magnetic Properties of cobalt and nickel Complexes of perezona and related ligands

Trabajo de integración curricular presentado como requisito para
la obtención del título de
Química

Autor:

Rosa Cecilia Medina Chalacan

Tutor:

Juan Pablo Saucedo Vázquez, Ph.D.

Urcuquí, febrero 2020

SECRETARÍA GENERAL
(Vicerrectorado Académico/Cancillería)
ESCUELA DE CIENCIAS QUÍMICAS E INGENIERÍA
CARRERA DE QUÍMICA
ACTA DE DEFENSA No. UITEY-CHE-2020-00006-AD

Er
en
int

En la ciudad de San Miguel de Urququí, Provincia de Imbabura, a los 28 días del mes de febrero de 2020, a las 09:30 horas, en el Aula CHA-01 de la Universidad de Investigación de Tecnología Experimental Yachay y ante el Tribunal Calificador, integrado por los docentes:

Presidente Tribunal de Defensa	Dr. CAETANO SOUSA MANUEL , Ph.D.
Miembro No Tutor	Dr. MAKOWSKI , KAMIL , Ph.D.
Tutor	Dr. SAUCEDO VAZQUEZ, JUAN PABLO , Ph.D.

S
li
S
ti
F
E

Se presenta el(la) señor(ita) estudiante **MEDINA CHALACAN, ROSA CECILIA**, con cédula de identidad No. **2200097034**, de la **ESCUELA DE CIENCIAS QUÍMICAS E INGENIERÍA**, de la Carrera de **QUÍMICA**, aprobada por el Consejo de Educación Superior (CES), mediante Resolución **RPC-SO-39-No.456-2014**, con el objeto de rendir la sustentación de su trabajo de titulación denominado: **SYNTHESIS AND MAGNETIC PROPERTIES OF COBALT AND NICKEL COMPLEXES OF PEREZONE AND RELATED LIGANDS** , previa a la obtención del título de **QUÍMICO/A**.

El citado trabajo de titulación, fue debidamente aprobado por el(los) docente(s):

Tutor	Dr. SAUCEDO VAZQUEZ, JUAN PABLO , Ph.D.
--------------	---

Y
e

Y recibió las observaciones de los otros miembros del Tribunal Calificador, las mismas que han sido incorporadas por el(la) estudiante.

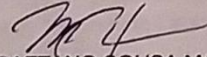
Previamente cumplidos los requisitos legales y reglamentarios, el trabajo de titulación fue sustentado por el(la) estudiante y examinado por los miembros del Tribunal Calificador. Escuchada la sustentación del trabajo de titulación, que integró la exposición de el(la) estudiante sobre el contenido de la misma y las preguntas formuladas por los miembros del Tribunal, se califica la sustentación del trabajo de titulación con las siguientes calificaciones:

Tipo	Docente	Calificación
Presidente Tribunal De Defensa	Dr. CAETANO SOUSA MANUEL , Ph.D.	9,7
Tutor	Dr. SAUCEDO VAZQUEZ, JUAN PABLO , Ph.D.	9,8
Miembro Tribunal De Defensa	Dr. MAKOWSKI , KAMIL , Ph.D.	9,9

Lo que da un promedio de: **9.8 (Nueve punto Ocho)**, sobre 10 (diez), equivalente a: **APROBADO**

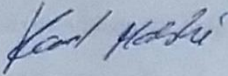
Para constancia de lo actuado, firman los miembros del Tribunal Calificador, el/la estudiante y el/la secretario ad-hoc.


MEDINA CHALACAN, ROSA CECILIA
Estudiante

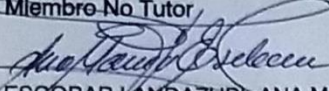

Dr. CAETANO SOUSA MANUEL , Ph.D.
Presidente Tribunal de Defensa


Dr. SAUCEDO VAZQUEZ, JUAN PABLO , Ph.D.
Tutor





Dr. MAKOWSKI, KAMIL, Ph.D.
~~Miembro No Tutor~~



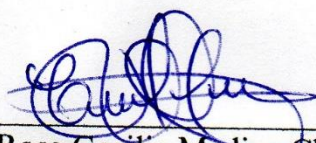
ESCOBAR LANDAZURI, ANA MARIA
Secretario Ad-hoc



AUTORÍA

Yo, Rosa Cecilia Medina Chalacan, con cédula de identidad 2200097034, declaro que las ideas, juicios, valoraciones, interpretaciones, consultas bibliográficas, definiciones y conceptualizaciones expuestas en el presente trabajo; así cómo, los procedimientos y herramientas utilizadas en la investigación, son de absoluta responsabilidad de la autora del trabajo de integración curricular. Así mismo, me acojo a los reglamentos internos de la Universidad de Investigación de Tecnología Experimental Yachay.

Urcuquí, Febrero 2020.



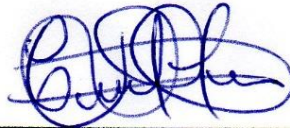
Rosa Cecilia Medina Chalacan
CI:2200097034

AUTORIZACIÓN DE PUBLICACIÓN

Yo, Rosa Cecilia Medina Chalacan, con cédula de identidad 2200097034, cedo a la Universidad de Tecnología Experimental Yachay, los derechos de publicación de la presente obra, sin que deba haber un reconocimiento económico por este concepto. Declaro además que el texto del presente trabajo de titulación no podrá ser cedido a ninguna empresa editorial para su publicación u otros fines, sin contar previamente con la autorización escrita de la Universidad.

Asimismo, autorizo a la Universidad que realice la digitalización y publicación de este trabajo de integración curricular en el repositorio virtual, de conformidad a lo dispuesto en el Art. 144 de la Ley Orgánica de Educación Superior

Urcuquí, Febrero 2020.



Rosa Cecilia Medina Chalacan
CI: 2200097034

Dedicatoria

Dedico este trabajo de tesis a mi familia y a mis amigos que me apoyaron y animaron durante mis momentos más desafiantes aquí en la Universidad de Investigación de Tecnología Experimental Yachay Tech

Rosa Cecilia Medina Chalacan

Agradecimiento

Quiero agradecer especialmente a mi asesor, el Ph.D Juan Pablo Saucedo por su actitud de compromiso con la investigación, me guió mucho, en particular su paciencia y ánimo.

Me gustaría agradecer a mis padres que siempre me dan ejemplo de buenos valores y la guía correcta para mi vida. Agradezco a mi tía Janneth Medina por su dirección y apoyo, siempre. Por último, quiero mostrar mi más profundo agradecimiento a todas las personas que me ayudaron durante toda la carrera; sin su ayuda, terminar la carrera y realizar mi trabajo de tesis no hubiera sido posible de lograr.

Rosa Cecilia Medina Chalacan

Resumen

La perezona es un sesquiterpeno benzoquinona de origen natural, útil para estudiar los sistemas de oxidación-reducción. Este compuesto se encuentra en las raíces del género *Perezia*, entre las cuales se encuentra la especie *Perezia multiflora*. En Ecuador, *Perezia multiflora* es una planta medicinal conocida como "escorzonera". El efecto citotóxico de la perezona se ha evaluado contra varias células cancerosas. A medida que los metales modifican las propiedades de varios medicamentos, los complejos de metales de transición que contienen ligandos de quinona se han utilizado en medicamentos contra el cáncer y contra otras enfermedades. La capacidad de unión de la perezona a los metales y su capacidad de experimentar reacciones de oxidación-reducción permite jugar una actividad esencial en los sistemas biológicos.

En este trabajo, mediante el uso de TLC, UV-Vis se observó la banda característica de la perezona y en el análisis de espectroscopia UPLC-MS se encontró la presencia de perezona en especies de *Perezia multiflora*. Las propiedades redox de estas quinonas también se confirmaron mediante el uso de potenciómetro. Posteriormente, la síntesis de los complejos de cobalto y níquel con perezona se llevó a cabo y se caracterizó mediante espectroscopia UV-VIS. Los resultados obtenidos mostraron que el complejo níquel-perezona tiene una coordinación 1: 2, mientras que el complejo cobalto-perezona mostró una coordinación 1: 1. Por otro lado, la espectroscopia EPR en estos compuestos mostró interacción hiperfina para el complejo de níquel-perezona, aunque los complejos de níquel se caracterizan por ser EPR silenciosos. Además, una característica interesante en los espectros de EPR obtenidos del complejo cobalto-perezona, fue la falta de acoplamiento hiperfino.

Los estudios magnéticos realizados en esos complejos mostraron un comportamiento antiferromagnético y sus temperaturas de Neel muy bajas $T_N = 1.79$ para cobalto-perezona y para níquel perezona en $T_N = 1.99$. Del análisis, también se obtuvieron valores pequeños para la constante de Weiss, lo que indica una baja temperatura de transición entre el comportamiento paramagnético y antiferromagnético.

Palabras Clave: *Perezia multiflora*, perezona, complejo, níquel, cobalto, propiedades magnéticas

Abstract

Perezone is a natural sesquiterpene benzoquinone useful to study oxidation-reduction systems. This compound is found in the roots of the *Perezia* genus, among which is the *Perezia multiflora* species. In Ecuador, *Perezia multiflora* is a medicinal plant known as "escorzonera". The cytotoxic effect of perezone has been evaluated against several cancer cells. As metals modify the properties of several drugs, transition metal complexes containing quinone ligands have been used in anticancer drugs and against other diseases. The binding ability of perezone to metals and its capacity to experience oxidation-reduction reactions allows playing an essential activity in the biological systems.

In this work, through TLC, UV-Vis is observed the characteristic band for perezone and UPLC-MS analysis was found the presence of perezone in *Perezia multiflora* species. The redox properties of this quinones was also confirmed through the use of Potentiostat. Subsequently, the synthesis of Cobalt and Nickel complexes with perezone was carry on and characterized through UV-VIS spectroscopy. The results obtained showed that Nickel-Perezone complex has a coordination 1:2, while Cobalt-Perezone complex showed a coordination 1:1. On the other hand, EPR spectroscopy on those compounds showed hyperfine interaction for Nickel- Perezone complex although Nickel complexes are characterized for being EPR silent. Furthermore, an interesting characteristic on the EPR spectra obtained from the Cobalt-Perezone complex, there is a lack of hyperfine coupling.

The magnetic studies carry on those complexes showed an antiferromagnetic behavior and their Neel temperatures very low $T_N= 1,79$ for Cobalt-Perezone and for Nickel Perezone a $T_N=1,99$. From the analysis, also was obtained small values for Weiss constant indicating low transition temperature between paramagnetic and antiferromagnetic behavior.

Keywords: *Perezia multiflora*, perezone, complex, nickel, cobalt, magnetic properties

1.	Introduction and Justification	1
1.4	Importance of quinones chemistry	2
1.1.1	Quinones in nature	4
1.1.2	Some typical application of quinone compounds	4
1.2	<i>Perezia Multiflora</i> Less Specie	5
1.2.1	Perezone	6
1.3	Brief introduction to quinone coordination compounds	7
1.4	Electronic Paramagnetic Resonance (EPR) Spectroscopy	9
1.4.1	Electron Spin in Magnetic Field (Zeeman Effect)	9
1.4.2	Lande splitting factor (g factor)	10
1.5	Molecular Magnetism	11
1.1.1	Curie Law	12
2.	Hypothesis and objectives	14
2.1	Hypothesis	14
2.2	General Objective	14
2.3	Specific Objectives	14
3.	Materials and Methodology	15
3.1	Materials	15
3.1.1	Vegetal Material	15
3.1.2	Reactants and equipment	16
3.2	Perezone isolation	16
3.2.1	Extract preparation	16
3.2.2	Thin Layer Chromatography (TLC)	17
3.3	Structural identification of perezone	18
3.3.1	UV-VIS analysis	18
3.3.2	Ultra Performance Liquid Chromatography (UPLC)	19
3.3.3	Electrochemical characterization	19
3.4	Synthesis and characterization of perezone complexes	19
3.4.1	UV-VIS Perezone complex analysis	19
3.4.2	Magnetism and EPR spectroscopic characterization	20
4.	Experimental results and discussion	21
4.1	Obtaining extracts from Escorzonera plant	21
4.2	Thin layer chromatography of the extracts	22
4.3	Chromatographic fractionation and recristalización	23
4.4	Structural Identification of perezone	26

4.5	Synthesis and structural identification for nickel and cobalt-perezone complexes	31
4.6	EPR spectroscopy for cobalt and nickel-perezone complexes	33
4.7	Magnetism for nickel and cobalt complexes	37
4.	Conclusion	42
5.	Bibliography	44

1. Introduction and Justification

It is well known that ancient civilizations used plants in order to treat several diseases; nowadays, some of those plants are still used in traditional medicine. Furthermore, those plants are also of great importance for the investigation of its active compounds. The investigation on those active compounds is done in order to prove its effectiveness and synthesize stronger drugs or other chemical compounds such as compounds with valuable magnetic properties. Among the plants used for phytochemical investigation is the genus *Perezia* which belongs to botanical family *Asteraceae*, and this is one of the most important family due to its rich chemistry in secondary metabolites¹. The genus *Perezia* had been divided into two sections: *Acourtia* and *Euperezia*, from central-north America and South America, respectively. Moreover, from genus *Perezia* are known about 85 species, from which the North American species have been studied chemically in detail, but South American species have seldom been studied².

In Ecuador, there is a great diversity in plants used with medical purposes; one of those plants is *Perezia multiflora*, commonly known as “escorzonera”. Some of the uses that this plant has in traditional medicine are: treat pharyngitis, heal teeth and throat injuries, also is used as diuretic, febrifuge, analgesic, anti-inflammatory, and to treat backache, stomach ache, and diarrhea³. Also, it possesses an antileishmanial activity. There is a difficulty for the conservation of this plant and others with critical therapeutic properties because their natural populations tend to scarce. They have been under continuous survival risk as effects of climate change and also because of anthropogenic activities.⁴ The knowledge generated from this study could contribute to making aware of the sustainable development and conservation of this species.

There is a natural secondary metabolite known as perezone (Figure 1.1) which was first isolated in 1852 by Leopoldo Rio de la Loza from roots of a species of the genus *Perezia*, and it was named pipitzahoic acid. Perezone belongs to a group of compounds of natural origin, quinones, which accomplish a significant role in the process of electron transfer which is relevant for life, such as photosynthesis.⁵ Several North America species from *Perezia* genus have been used to extract perezone and those studies suggest that the presence of this quinone in plants give them a laxative and purgative property.⁶ As the

genus *Perezia* is known for containing perezone, studies in north America species have been developed for its interesting redox properties that could be applicable in the pharmaceutical industry and others⁷.

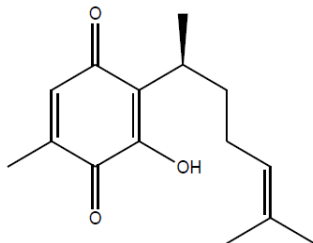


Figure 1.1 Perezone structure

This important secondary metabolite possesses the properties of a quinone: it is a crystalline substance with a deep orange color, and also have three redox states: totally oxidized, semiquinone, and totally reduced quinone. These properties make perezone useful for biological activity, and with its acidic protons, have a meaningful electrochemical behavior.⁴ This capacity to be wholly oxidized or reduced allow perezone to participate in the electron transport chain, and due to its midpoint redox potential that indicates a high affinity to electrons, this compound can inhibit the oxygen consumption in the electron transport chain⁸.

Due to these redox properties, in the last quarter-century, research has been grown towards the understanding of coordination compounds containing quinone ligands and its properties.⁹ Therefore, several coordination compounds containing ligands with those redox properties have been synthesized and studied. The understanding of its structural, electrochemical, and magnetic properties has been increased. This study has the objective to isolate and characterize perezone from roots of *Perezia multiflora*; and use it as an organic ligand for nickel and cobalt complexes. Finally, characterize the synthesized compounds and their resulting magnetic properties.

1.4 Importance of quinones chemistry

Quinones are conjugated cyclic carbonyl compounds of 6 members naturally occurring.¹⁰ There are two important forms in which the carbonyl groups are oriented: para-quinone (1,2-benzoquinone) and orto-quinone form (1,4-benzoquinone)¹¹. Those compounds are impressive, mainly because of its rich chemistry. Quinones undergo a reversible oxidation-reduction process that involves multiple π -conjugated electrons from carbonyl

groups.^{12, 13} Apart from its redox properties, the color is also a relevant characteristic of this compound. The ability of quinones to absorb ultraviolet and visible light energy makes possible their yellowish, orange or reddish pigmentations.¹⁴

The redox mechanism of quinones affords high energy densities comparable to those of inorganic materials without a change in structure.¹³ The three possible oxidation states of quinone compounds in neutral aprotic media, represented in Figure 1.2, are a) the fully oxidized quinone (Q), b) one-electron reduction to form radical anion (Q^{•-}) semiquinone, and c) two-electron reduction to form a dianion (Q^{2•-}) catechololate.¹³

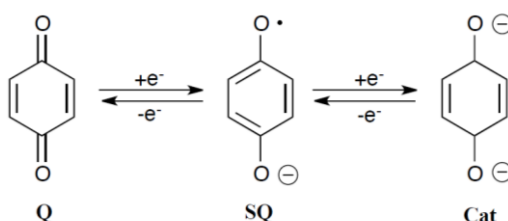
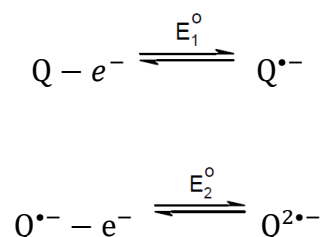


Figure 1.2 Basic structure of quinones, semiquinone, and catechololate

Several biological processes depend on the electron transfer reactions that involve the Q/SQ/Cat redox series.^{13, 15} The amount of Q, Q^{•-} or Q^{2•-} is dependent on the pH of solution and presence of oxygen.¹³ These three forms of quinone would be present in the same quantities in aqueous solution at pH 7.¹³



Most reactions of quinones involve oxidation or reduction of the quinoid ring, and the kinetics of addition reactions are related to the redox potential of couple Q/Q^{•-} (E^o₁) and Q^{•-}/Q^{2•-} (E^o₂), which are generally quasi reversible reactions.¹⁶ The measure of E^o and electron density is modified when there are substituents on the quinone ring.¹³ Quinones without a side chain have high electrophilicity. Electrophilic activity decreases with a side chain.¹² Therefore, E^o becomes more negative with donating electron groups, hindering the reduction of those species¹³.

All possible structural diversity of quinones undergoes nucleophilic attack and metabolic reduction. But the chemical difference of those structures lies on a quantitative measure of how reactive it is.¹⁴

1.1.1 Quinones in nature

Many quinones are interesting secondary metabolites found widespread in natural products from plants, fungi, and bacteria.^{6, 12, 14} Those secondary metabolites can be synthesized via the shikimate or polyketide pathways. Mammals lack these pathways, but they can synthesize quinones by oxidative metabolism of endogenous substances.¹⁴

Quinones generally found in all respiring animals and plants act like free-electron transport in photosynthesis and respiratory electron transport chains¹⁷. The physicochemical properties of these compounds are the responsible of the overall biological activity.¹²

As secondary metabolites, they also play an essential role in cellular defense, inhibiting bacterial, fungal, and parasite growth.⁴ However, quinones have been studied for their cytotoxic activity and founded its application as effective anticancer drugs¹⁸. Therefore, these compounds can be either effective antibacterial, anticancer, or cytotoxic agents. These essential activities are related to the easy electron and proton transfer process during quinone-catecholate interconversion. This interconversion principally motivates electrochemical studies.¹⁶

Generally, oxidation reactions of quinone compounds are associated with the production of O^{2-} and H_2O_2 . Another mechanism for their toxicity lies in its electrophilic activity, such as the reductive addition.¹³ Therefore, quinones have been employed as examples models to study cellular mechanisms of chemical-induced toxicity¹⁴.

1.1.2 Some typical application of quinone compounds

The medicinal properties of quinones have been well recognized, and the extracts of plants that contain those compounds show activity against several diseases. As an example, since antiquity, extracts of plants containing quinones such as rhubarb and aloe have been used as purgatives.¹⁴ Besides, quinone compounds naturally occurring are of great interest as active redox materials for electrical energy storage. The advantage that provides quinones for those devices is low environmental load and cost-effectiveness.¹⁹

This compound also has been served as hormones and pigments for a long time.¹⁷ As an example, the pigment known as Henna is a paste made from leaves of *Lawsonia inermis*, that is reddish-orange, used since antiquity as cosmetic and coloring matter.¹⁴

1.2 *Perezia Multiflora* Less Specie



Figure 1.3 *Perezia Multiflora* Taken from Tropicos.org

The genus *Perezia* has been divided taxonomically into two sections: *Acourtia* and *Euperezia*. Section *Acourtia* is distributed in North America, while section *Euperezia* extends in South America.²⁰ The South American genus *Perezia* has about 30 species that have been poorly studied.² Previous investigations in some high Andean plants belonging to *Euperezia* section have found the presence of secondary metabolites with therapeutic properties.²¹ Especially in Mexican traditional medicine, the woody roots from some of these species have been used since antiquity to prepare a laxative beverage. Detail will be given later about an essential secondary metabolite, first named as pipitzahoic acid, responsible for this therapeutic activity.²⁰

A plant of this genus that presents interesting characteristics is *Perezia multiflora* (Figure 1.3), whose common name is Escorzonera or Chancoruma. This plant is generally found at an altitudinal range between 2500-4500 masl in South America. This plant measures up to 30 cm high, and the flowers are white and have many thorns.²² This plant is used in traditional medicine to treat several ailments such as backache, stomach ache, flu, fever,

cough, bronchitis, tuberculosis, and diarrhea. Also, this plant is helpful for its diuretic, analgesic, anti-inflammatory activity and to heal teeth and throat injuries.³

Perezia multiflora species can be found in the following provinces: Azuay, Cañar, Carchi, Chimborazo, Cotopaxi, Napo, Pichincha, Tungurahua²²

Table 1.1.1 Taxonomy of Escorzonera plant. ²²

Kingdom	Plantae
Order	Asterales
Family	Asteraceae
Genus	<i>Perezia</i>
Specie	<i>Perezia multiflora (Humb.y Bonpl.) Less.</i>

Studies on this plant have demonstrated the anti-inflammatory activity from the extract for tail and leaves against *Staphylococcus aureus* and *Bacillus subtilis*.²¹ Moreover, its antimicrobial activity has been evaluated in order to treat common infections, illnesses such as respiratory, skin, urinary, and stomach ache.³ The plants collected for that study were from Cordillera Blanca, Peru.

The secondary metabolites found in this species were coumarins that have been isolated from the roots of this plant, using hexane solvent for extraction.²³ The presence of seven new isocedrenes and others sesquiterpenes esters was confirmed from methanol-diethyl ether-petrol (1:1:1) extraction in *Perezia multiflora* collected from Bolivia.²

1.2.1 Perezone

The secondary metabolite named above, the pipitzahoic acid, currently is known as perezone [2-(1,5-dimethyl-4-hexenyl)-3-hydroxy-5-methyl-1,4-benzoquinone] with molecular weight 248.3 Dalton.²⁴ This secondary metabolite was isolated for the first time in Mexico in 1852, by Leopoldo Río de La Loza.^{1, 5, 18} Further studies have been found that perezone is fairly abundant in the roots of *Perezia cuernavacana* species. The structural formula of this compound is shown in Figure 1.1. This compound is a sesquiterpene quinone with a double bond at remote position.²⁴ The unsaturated chain in

the planar quinoid ring at C(2) adopts an extended form and is oriented out of plane of the quinone ring,²⁵ it changes E° that is associated with its important biological activity.²⁴

As a quinone compound, perezone possesses properties such as: being a crystalline substance with deep orange color, and its redox properties. Also, perezone may cause cells death because of a huge generation reactive oxygen species.¹⁸ Its biological activity is related to their redox and acid-base chemistry. Perezone, which contains acidic protons, displays important electrochemical behavior.⁴ This exhibits oxido reduction characteristics which suggest that the compound can be used for studies of electron transport.⁸

Therefore, perezone can be employed as a pigment²⁶ and it may form coordinated compounds with metals to produce other pigments of different colors.²⁰ In addition, this compound has important pharmacological activities.²⁷ It can be used as an antimicrobial agent²⁰ and had been used in the traditional Mexican medicine as laxative and antiparasitic.⁴ Furthermore, this cytotoxic quinone can be taken advantage as medicine against several cancer cell lines such as myeloblastoid leukemia.²⁸

Even though the potential applications of this secondary metabolite, its isolation from *Perezia* species is very poor. The yield of perezone ranges from 2 to 8% of the dry weight plants, depending on the methods used for extraction, the plant growth stage, season when the plant is collected, and natural stress conditions.²⁰ Other factor that affect the isolation of enough amounts of perezone for industrial purposes are: the small populations of *Perezia* species (some of them are in danger of extinction) and the currently methods for cultivate *Perezia* have failed.²⁰

1.3 Brief introduction to quinone coordination compounds

Research about quinone complexes has increased in recent years due the interest in its electrochemical and magnetic properties.⁹ Generally, those quinone complexes are curious examples of paramagnetic compounds.²⁹ The main difference between ortho-quinones comes from its chelating nature. For ortho-quinones there is a common chelating binding site whereas for para-quinones there are usually additional donors for chelation.³⁰ The two possible interactions between para-quinones and the metal are: a) metal coordinated to the π -system of the quinone aromatic ring, including cases of η^5 -

semiquinone and η^4 -quinone coordination; and b) metal interact with the quinone via a sigma-bonding to the oxygen atoms (Figure 1.4).¹⁷

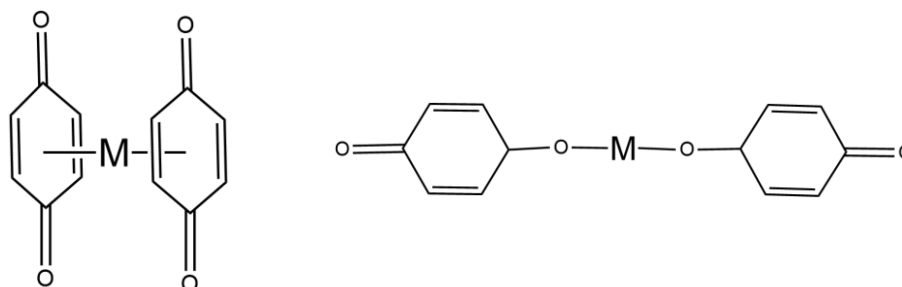


Figure 1.4 Design of the metal complex with quinone ligand as (left) metal coordinated to the π -system of the quinone ring and (right) metal interacting coordinated via a sigma-bonding to the oxygen atoms.

Quinones have the capacity to bind to metals in its three oxidation states: quinone, semiquinone and catechol.⁹ Quinone as a ligand that change its oxidation states is considered an non-innocent ligand. Hence, as a transition metal may have different oxidation states, the behavior of an non-innocent ligand is analogous to it.³¹ Therefore, the assignment of oxidation states for those coordination compounds is no a priori obvious, due to the change in oxidation state of the quinone ligand.³⁰

A multi-redox system with a variety of structural designs is formed when non innocent ligand coordinates to a transition metal depicted in Figure 1.5. Aside from the direct coordination of the redox site of ligand and the transition metal, there may appear interaction through bond or through space.³²

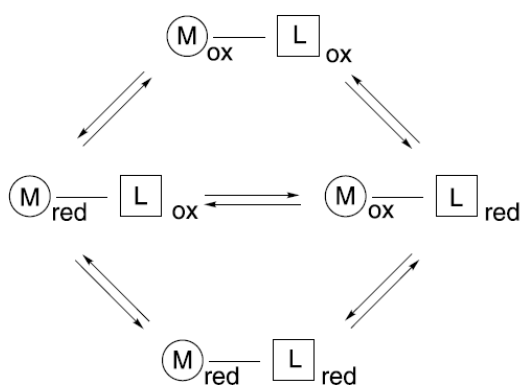


Figure 1.5 Multi-redox system for the coordination between transition metal and non-innocent ligand. Taken from Hirao.

1.4 Electronic Paramagnetic Resonance (EPR) Spectroscopy

This technique is analogous to the NMR spectroscopy, as both work with interaction of electromagnetic radiation with magnetic dipole moments. The main difference with EPR spectroscopy resides in that magnetic moments arise from movement of unpaired electrons in the molecule.³³

The experiment is carry on maintaining fixed frequency, and the more usually band frequency is X(9.5 GHz).³⁴ When molecular systems with unpaired electrons are under external magnetic field they absorb electromagnetic radiation just with specific energy values. This radiation absorbed is related with possible electronic states and the possible electronic orientations of system spin.³³

A system that contains unpaired electrons responds to an applied magnetic field by introducing the Zeeman effect and the g -factor.³⁵

1.4.1 Electron Spin in Magnetic Field (Zeeman Effect)

Electrons are characterized by an intrinsic mechanical angular momentum called spin. The electron spin can be in two states, usually indicated as α and β that corresponds to $m_s=+1/2$ and $m_s=-1/2$ respectively. The orientation of the angular momentum varies in space, but not in the magnitude. Under the presence of a magnetic field, the energy separation between those spin states is due to the presence of magnetic moment for each one.³⁴

This splitting of the electron spin energy level when a magnetic field is applied is called the Zeeman effect. This magnetic dipolar transition between those two spin states is produced when microwave energy matches its energy difference. The energy difference between the two resultant states is given by.³⁴

$$h\nu = \Delta E = g\mu_B B_0$$

Where g is the Lande splitting factor that for a free electron $g=2.002319$, μ_B is the Bohr Magneton, and B_0 is the magnetic field applied. The simplest energy-level diagram for a

particle of spin 1/2 in a magnetic field is shown in Figure 1.6. E_α and E_β represent the energies of the $m_s \pm 1/2$ states.³³ The spin states α and β have the same energy in the absence of magnetic field ($B_0=0$), and the splitting of the energy levels appears in the presence of an external magnetic field ($B_0 \neq 0$).

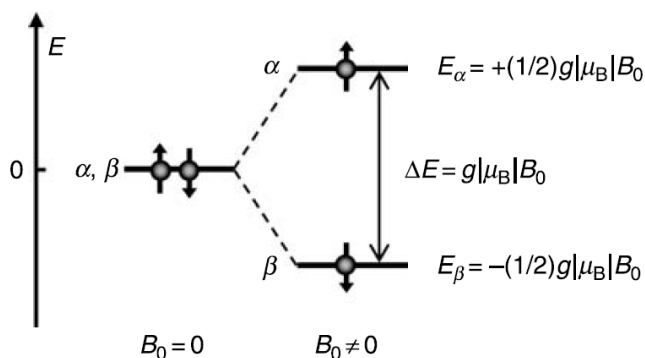


Figure 1.6 Energy states of an unpaired electron in an applied magnetic field B_0 .

1.4.2 Lande splitting factor (g factor)

The value of g factor mainly depends on the environment of the unpaired electron; it also varies with the physical state of the sample and the orientation of the molecule with respect to the applied magnetic field. Generally, the g value for organic radicals are pretty close to the free electron g value, as far as they are composed by “light” atoms. In contrast, the g value is larger for metal complexes, where the electrons move in proximity to a heavy atom nucleus.³⁴

There is a variation in the g value due to the spin–orbit coupling, especially when heavier elements are involved. In EPR spectra is expected to extract information of intra- and intermolecular interactions, molecular configuration, site symmetry, and the nature of neighboring atoms.³³

The local symmetry at any unpaired-electron center is classified in order of decreasing said local symmetry:³⁶

a) Cubic. This occurs when there is no anisotropy in g values, means that $g_{11}=g_{22}=g_{33}$. For d transition metal compounds this would only occur for perfectly cubic, octahedral or tetrahedral stereochemistry.

b) Axial. A molecule has axial g values when two of the principal g values are equal: $g_{11}=g_{22}\neq g_{33}$. As for isotropic systems those have certain molecular geometries.

c) Rhombic. This is the general case, where g values are $g_{11}\neq g_{22}\neq g_{33}$.

This knowledge of the behavior for a single isolated paramagnet is significant to understand the spectra from random oriented batch of paramagnets, which are found in experiments.³⁶

1.5 Molecular Magnetism

Measurements of magnetic properties are useful to characterize different molecular systems. All materials are affected under a magnetic field, that is to say all materials possess magnetic properties. They are mainly classified in diamagnetic and paramagnetic substances. Diamagnetic elements have all electron spin-paired, and those are repelled by an applied magnetic field. Substances with unpaired electrons are paramagnetic, and those are attracted by the magnetic field.³⁷ Paramagnetic materials, according to ordering of spins, can be subdivided in simple paramagnetic, ferromagnetic, ferrimagnetic and antiferromagnetic materials³⁷. The main magnetic features of those materials are the coupling between magnetic orbitals and their overlap.³⁵

Every charged particle carry an angular moment associated with a magnetic moment. The magnetic moment of an ion has contribution of the spin and orbital motion of its electrons. The value of magnetic moment is the sum of this two contributions.³⁴ However, a non-spherical environment will present just the contribution from the spin only magnetic moment.

$$\mu_{eff} = \mu_{s.o} = 2\sqrt{S(S+1)} = \sqrt{n(n+2)}BM$$

The contribution from the orbital angular momentum to the magnetic moment is given by:

$$\mu_{eff} = \sqrt{L(L+1) + 4S(S+1)}$$

The magnetic data is reported in literature with the magnetic susceptibility represented by χ , which indicates the Magnetization, M , degree of matter in response to a magnetic field, H .

$$\chi = \frac{M}{H}$$

1.1.1 Curie Law

The study of the effect of temperature on magnetic properties, found that for several paramagnetic substances, χ and temperature T are inversely proportional.³⁷ This is known as the Curie law:

$$\chi = \frac{C}{T}$$

Where C is the curie constant.

$$C = \frac{Ng^2\mu_B^2 S(S+1)}{3kT}$$

N is Avogadro number, μ_B is the Bohr Magnetron and k is the Boltzman constant. Generally when plotting χ vs T the results obtained are no so clear to differentiate between the order of paramagnets substances. Therefore, it is more common to obtain a better analysis plotting χT versus T . Following the Curie law, this plot gives a line parallel to the T axis. Also, for a plot of χ^{-1} versus T obeying the Curie law a relationship appears and goes to zero at $T = 0$, and the slope of the curve provides C . However, is common to find deviations from this linear behavior. Magnetic materials such as ferromagnetic and antiferromagnetic become paramagnetic metal at a temperature known as Curie temperature or Neel temperature respectively. Then, a correction for the Curie law is present as:³⁵

$$\chi = \frac{C}{T - \theta}$$

This expression is the Curie–Weiss law, where θ is an adjustable parameter, called Curie–Weiss constant.³⁵ In order to obtain C and θ is appropriate to fit χT versus T because it

gives different values for the constants.³⁵ A model to recognize the kind of magnetic substance is depicted in Figure 1.7. The χ^{-1} versus T plot gives the θ value where the straight line intercepts abscissa. If θ is positive the interaction between molecules and ions is ferromagnetic, while if θ is negative the interaction is antiferromagnetic.³⁷

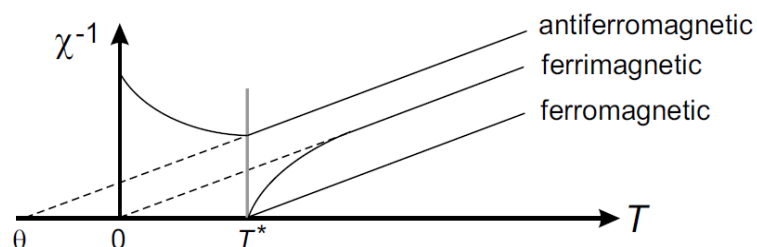


Figure 1.7 Typical behavior of ferrimagnetic, ferromagnetic and antiferromagnetic materials visualizing in an inverse of magnetic susceptibility versus temperature plot. Taken from Getzlaff.³⁸

2. Hypothesis and objectives

2.1 Hypothesis

It is expected presence of perezone, or other secondary metabolite similar to this quinone, in the roots of *Perezia Multiflora*. Furthermore, finding interesting magnetic properties of nickel and cobalt coordination compounds using this quinone as ligand. The products obtained from the reaction will be characterize with habitual spectroscopic characterization UV-Vis, EPR, Magnetic Susceptometer and UPLC-MS spectroscopy.

2.2 General Objective

Isolate and identify perezone from roots of *Perezia Multiflora*, and synthesize complex compounds with nickel and cobalt, using this isolated compound as an organic ligand. Study the magnetic behavior of the resulting compounds.

2.3 Specific Objectives

1. Isolate and identify the presence of perezone in different extracts (dichloromethane and hexane) from roots of *Perezia multiflora*.
2. Characterize the structure of the isolated quinone compound with UV-Vis and UPLC-MS spectroscopy and evaluate the electrochemical properties of quinones with Cyclic voltammetry technique.
3. Use perezone (quinone isolated from *Perezia multiflora* as a ligand in the synthesis of nickel and cobalt complexes.
4. To know the magnetic properties of the obtained nickel and cobalt complexes through EPR spectroscopic techniques.
5. To know the magnetic behavior of the perezone complexes, through studies on the samples, using the magnetic susceptometer.

3. Materials and Methodology

3.1 Materials

3.1.1 Vegetal Material

The biological material, roots of *Perezia multiflora* (Figure 3.1), was obtained from a market in Tungurahua province (February 2019). The taxonomic determination of this plant was realized through the available literature.



Figure 3.1 Biological material: Complete plant, Perezia multiflora, bought in market of the Tungurahua province

3.1.2 Reactants and equipment

REAGENTS	EQUIPMENT
Distilled water N.S	Heating mantle LASSCO 150W
Ethanol (99%. Fisher chemical)	UPLC-MS ACQUITY UPLC® I-Class
Hexane (98%. Fisher chemical)	Perkin-Elmer UV/VIS/NIR Lambda 1050 Spectrometer
Dichloromethane (99%. Honeywell)	Grain mill
Ethyl acetate (99%. Fisher chemical)	EPR ELEXSYS E500 Bruker spectrometer
Acetone (99.6%. Fisher chemical)	Stove POL-EKO-APARATURA SP-J
Iodide	Analytical Balance OHAUS Explorer
Silica gel 60	Potentiostat- Galvanostat Autolab Methrom
Cobalt chloride hexahydrate (98%. TCI America)	Susceptometer MPMS (Magnetic Properties Measurements System)
Nickel chloride hexahydrate (99%. Puratronic)	
Petroleum ether (distilled recovery)	
Dimethyl sulfoxide (Fisher Chemical)	
Ethyl ether (99% Fisher Chemical)	

Table 1. Detail of materials, reagents, and equipment used in the development of the present study

3.2 Perezona isolation

3.2.1 Extract preparation

The methodology used for the preparation of extract was according to a previously reported in literature¹. Before to move to the extraction process step, the roots from escorzonera plant were cleaned thoroughly and cut in small pieces. Water and a small brush were used to wash the roots and eliminate impurities and stranger particles from it. Then, the roots were put on paper and left for five days on the stove at 30°C in order to not exposed it to light and avoid moiety. Once the roots were dried, they were triturated with a grain mill.

The triturated sample was weighted, and appropriate portions were transferred to a filter chamber to introduce in the Soxhlet apparatus. For the extraction, two different solvents were used, one extraction (15,95g) was with 120 mL of hexane and the rest (200,68g) with 380 mL dichloromethane. For each load in the filter chamber were realized three-four cycles in the Soxhlet apparatus until solvent at siphon arm appears colorless.



Figure 3.2. Development of drying *Perezia multiflora*'s roots: a) Washing the roots, b) Roots of *Perezia multiflora* already washed and dried, c) Crushing of dried roots, d) The whole sample of crushed roots.

3.2.2 Thin Layer Chromatography (TLC)

For this study was used TLC due to its high capacity to detect active biological compounds making use of different methods to reveal the spots. Moreover, because it is helpful to a faster and efficient fractionation chromatographic process. A standard perezone crystallized was used in this and other analysis to compare and verify the presence of perezone in the *Perezia multiflora* species. The procedure was:

- 1) Three points were used to detect the presence of perezone: standard perezone crystallized, hexane extract and dichloromethane extract

- 2) As eluent for TLC was used diethyl ether-ethyl acetate (9:1) in the chromatographic chamber, where the plates were inserted and left to run the solvent. Finally, the chromatoplates were extracted, left to dry, and mark the spots observed.
- 3) The active components were identified using iodide revealed chamber (stem iodide), p-anisaldehyde stain, and also a UV lamp. Once the spots were revealed, we mark those, and the respective Rf values were calculated.

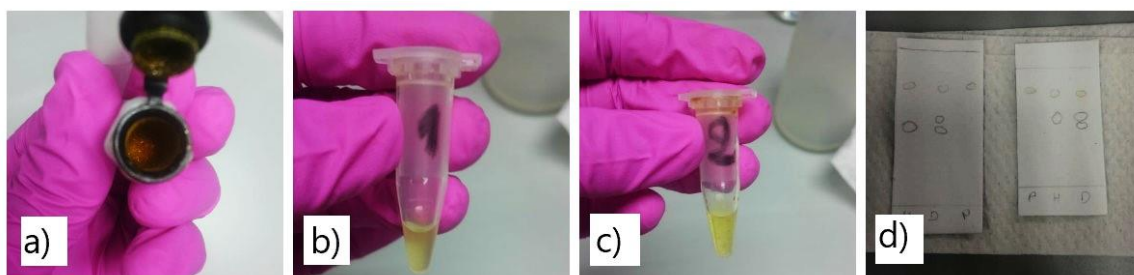


Figure 3.3. Materials for chromatographic analysis: a) Perezzone recrystallized for spot 1, b) hexane extract for spot 2, and c) dichloromethane extract for spot 3.

After the evaluation, the TLC results for the hexane and dichloromethane extract; the residue of both extracts were passed through column chromatography.

Silica gel was used as the stationary phase in the glass chromatography column. Gradient elution was carried out, beginning with diethyl ether-ethyl acetate (9:1) and increasing polarity for hexane extract, and a gradient elution beginning with petroleum ether-ethyl acetate (9:1) for dichloromethane extract. Then, TLC analysis was carried out for the fractions collected in order to supervise the adequate separation of substances and isolate perezzone from extracts. The chromatographic profile of the fractions was established after the analysis for TLC revealed under the UV-LIGHT developer, with iodide chamber and anisaldehyde revealer.

3.3 Structural identification of perezzone

3.3.1 UV-VIS analysis

Electronic spectrums for the dry dichloromethane and hexane extracts were obtained and compared with the spectrum of perezzone crystallized in order to ensure the presence of perezzone in the roots of *Perezia multiflora* species. The samples were dissolved in ethanol at 2 mM concentration each one to perform the UV-Vis analysis. Then, it was recorded in scans from 200 to 800 nm.

3.3.2 Ultra Performance Liquid Chromatography (UPLC)

UPLC-MS was used to determine the presence of perezone in extracts, and it was realized according to a methodology found in literature to comparing results.³⁹ This analysis was performed to dry fractions that showed the presence of perezone; these were dissolved in methanol at a concentration of 5 µg/mL. The analysis was performed with an Acquity UPLC maintained at 40 ° C, with an injection volume of 0.2 µL. The mobile phase constituted a gradient system of water acidified with 0.1% formic acid in water (A) and acetonitrile (B) in a flow constant of 0.25 mL/min. The ionization technique used was ElectroSpray Ionization-Mass Spectrometry (ESI-MS). The negative electrospray ionization (ESI) causes negative ions of perezone to predominate and be detected.

3.3.3 Electrochemical characterization

Cyclic voltammograms from perezone crystallized and DCM extract were obtained in order to compare and identify its characteristic electrochemical properties. The electrodes used within the electrochemical cell was carbon glass as a working electrode, Platinum as reference electrode and graphite as a counter electrode. The rate was at 50 mV/s. Lithium perchlorate (LiClO₄) was used as the supporting electrolyte at a concentration 0.2M, and the concentration of perezone was 2mM and in DMSO. The DCM dry extract for the analysis was at a concentration 2mM and with the same conditions as for perezone voltammogram.

3.4 Synthesis and characterization of perezone complexes

3.4.1 UV-VIS Perezone complex analysis

The method of concentration variation was used in order to find out the stoichiometric relationship in which nickel-perezone and cobalt-perezone complexes combined. Solutions of the same molarity were prepared for each salt and perezone extracted. Then, successive reactions were realized by varying the amount of ligand and metal, but the final volume was maintained.

For the first complex analysis, NiCl₂*(H₂O)₆ and perezone extracted (Pz) were prepared in ethanol as a solvent. For the second coordination compound analysis, CoCl₂*(H₂O)₆ and perezone extracted (Pz) were prepared in ethanol as a solvent. In order to check the

coordination of perezone with each metallic salt, the samples with different concentrations of perezone and metals were analyzed in a UV-Vis spectrophotometer, recorded in scans from 200 to 800 nm.

Once the stoichiometric relation is figured out, the nickel-perezone and cobalt-perezone complexes were prepared by general procedure at atmospheric pressure. The metallic salt and perezone were dissolved separately, using ethanol as solvent, stirred for several minutes until all they are dissolved. Then the metal and perezone solutions were mixed and also stirred. Once the color of solution did not change hydrochloric acid was added. The solution was filtrated to eliminate impurities and the solvent let to evaporate to obtain the crystals.

Table 3.1 summary synthesis of nickel-perezone complex

Reactant	Molar Mass (g/mol)	Mass used (g)	Mmol
Pz	248.32	2.03	8.17
NiCl ₂ *(H ₂ O) ₆	129.599	0.53	4.08

Table 3.2 summary synthesis of cobalt-perezone complex

Reactant	Molar Mass (g/mol)	Mass used (g)	mmol
Pz	248.32	0.998	4.02
CoCl ₂ *(H ₂ O) ₆	129.839	0.56	4.31

3.4.2 Magnetism and EPR spectroscopic characterization

EPR spectroscopy was carry out with a scan rate field between 2272 G to 4272 G. The equipment used was a Bruker ELEXYS E500 device from the USAI of the Faculty of Chemistry of the UNAM University. EPR measurements was realized in powder and water solution samples of the nickel-perezone complex and were realized in powder sample of cobalt-perezone complex. Magnetic properties of cobalt complexes were carry on at temperature 10K, and for nickel complexes, the study was realized at 10K and at

room temperature using X-band (9.4 GHz) y 100KHz modulation using 4102ST at a temperature 10K.

Magnetic measurements were made using a MPMS magnetometer (Magnetic Properties Measurements System) in which the magnetic susceptibility was determined in a temperature range of 2 to 300 K under an applied field of 5 T, as well as isothermal magnetic measurements of variable field magnetization in a range of ± 5 T to 2 K. Magnetic measurements at variable temperature and magnetic field were made using a Magnetometer (MPMS), for this, the sample was properly packed in a plastic capsule and subsequently placed inside the equipment in order to measure the magnetic properties of interest. In this way, the magnetization of the material at different temperatures in the range of 2 - 300 K was measured under a constant magnetic field H , of 1000 Oe, from these variables, the value of magnetic susceptibility given by the ratio M/H was calculated. It was graphing each measured value of the magnetic susceptibility at a certain temperature.

4. Experimental results and discussion

4.1 Obtaining extracts from Escorzonera plant

First, it was obtained a fine ground sample for the dry root of escorzonera plant. Then, 15.95 g of sample portions were transferred to the soxhlet apparatus to extract the secondary metabolite with hexane solvent. For dichloromethane solvent, the powder sample (200.68 g) was weighted, and with extraction was done it by the soxhlet apparatus in portions of 20 g. Hexane extract color was yellow, and for dichloromethane extract, a reddish-orange color appeared and it was quite thick, indicating a saturated solution (Figure 4.1).

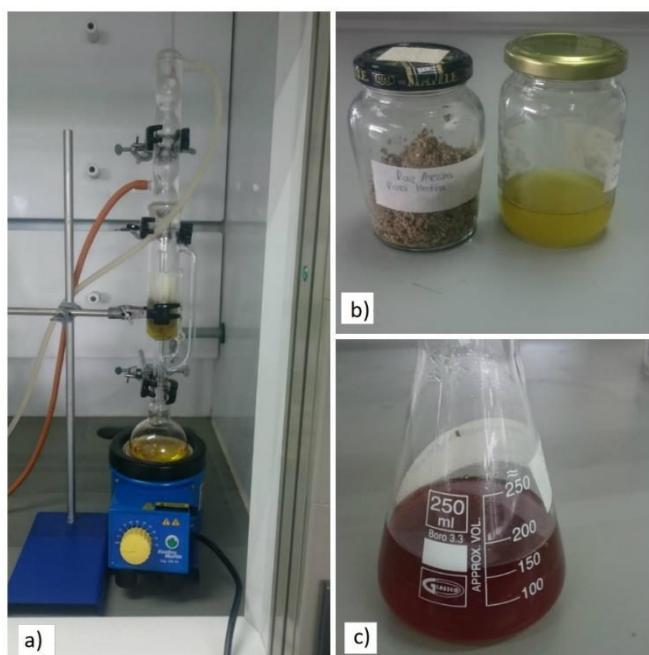


Figure 4.1. Extraction process: a) Assembly of the apparatus and run of the cycles with each solvent, b) roots residue and hexane extract, c) Dichloromethane extract.

DCM extract shows higher density than hexane extract, hence it is observed that this extract possesses more substances in solution. After the rotavaporation process, the dry residues for the hexane and dichloromethane extract, were yellowish-orange and reddish-brown, respectively. Both residues obtained had an oily texture. Hexane extract yielded 0.129 g, and dichloromethane extract yielded 1.987g that is a 0.8% and 1% for the plant extracts respectively.

4.2 Thin layer chromatography of the extracts

As described before, the hexane and dichloromethane extracts were analyzed by TLC in order to ascertain the presence of perezone and observe other compounds. Different results were obtained according to the visualizing technique used. With a UV lamp, just one spot was observed, with the same R_F (0.78) of the pattern of perezone, and with the iodide chamber, other spots appear for hexane and dichloromethane extracts (Figure 4.2).

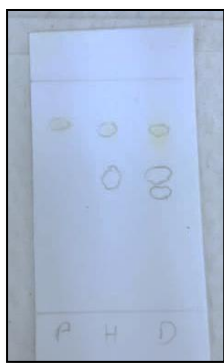


Figure 4.2. Chromatography of: hexane extract (H) and dichloromethane extract (D) compared with standard perezone crystallized (P). Mobile phase: diethyl ether-ethyl acetate 9:1 (v/v). Revelator: iodide chamber and UV- lamp.

Root extract	Detection	Experimental color	R _F value
Hexane extract	Light UV-Vis	Fluorescence Green	0.78
	Iodide camera	Orange-brown	0.58
Dichloromethane extract	Light UV-Vis	Fluorescence Green	0.78
	Iodide camera	Orange-brown	0.58
			0.49
Perezone	Light UV-Vis	Fluorescence Green	0.78

Table 4.1 R_F calculated from TLC plates when revealed with light UV-Vis and iodide camera, using hexane and dichloromethane extracts with a mobile phase: diethyl ether-ethyl acetate 9:1 (v/v).

The several spots observed in TLC plates from hexane and dichloromethane extracts indicated the need to carry on column chromatography. Also is observable that dichloromethane extract possesses other secondary metabolites than hexane extract, and Perezone crystallized had some impurity too. Dry residue from hexane extract was crystallized with hexane-acetone (9:1), and the residue obtained was still oily and weighed 0.072 g.

4.3 Chromatographic fractionation and recrystalización

The dry residues obtained from hexane and dichloromethane extracts were subjected to column chromatography (Figure 4.6). In order to improve the separation conditions, the change in eluent of mobile phase composition was used. Two chromatographic columns were made for residue obtained from dichloromethane extract. For the first sample, the

solvent gradient began with ether-ethyl acetate (9:1) and 15 fractions were obtained. After the analysis with TLC, the fractions which showed the presence of perezone were selected (3-6) and joined.

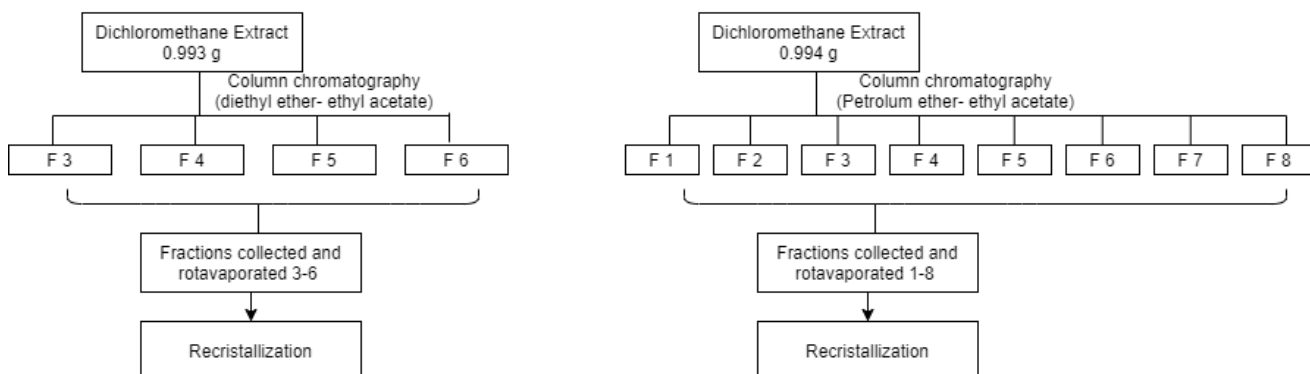


Figure 4.3 Flowchart with chromatographic fractionation steps of the dichloromethane extract from roots of *Perezia multiflora*.

The solvent gradient for the sample from dichloromethane residue began with petroleum ether-ethyl acetate (9:1). And 28 fractions were obtained, fractions (1-8) were joined, which showed the presence of perezone. Also, a mini-column chromatography was made for hexane extract. The solvent gradient for this sample begun with diethyl ether-ethyl acetate (9:1). After TLC analysis 7 fractions were obtained, the fractions (4-5) which showed the presence of perezone were joined.

After evaporated the selected fractions from dichloromethane extract under reduced pressure, these were recrystallized with hexane-acetone (9:1), and a reddish yellow oily residue was still obtained (Figure 4.7).

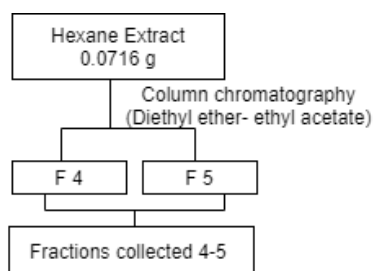


Figure 4.4 Flowchart with chromatographic fractionation steps of the hexane extract from roots of *Perezia multiflora*

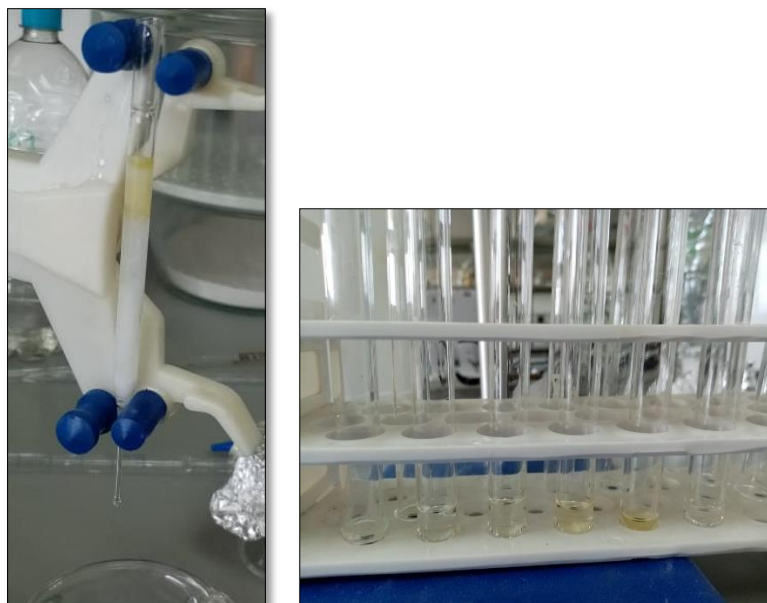


Figure 4.5. Mini chromatographic column for hexane extract: (left) Running the column chromatography, (right) Collecting the fractions from the column.



Figure 4.6. Column chromatographic process for dichloromethane extract: (left) Running the column chromatography, (right) Collecting the fractions from the column.

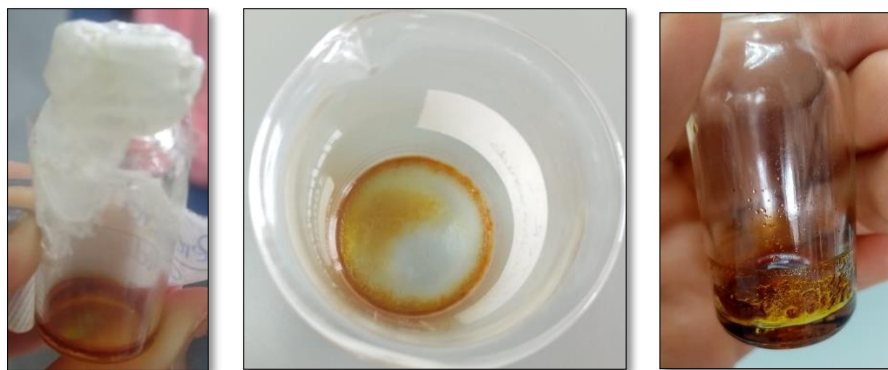


Figure 4.7. Dry residue from hexane extract (left), Dry residue from dichloromethane extract obtained from fractions in column chromatography of ether-ethyl acetate gradient (middle) and dry residue from dichloromethane extract obtained from fractions in column chromatography of petroleum ether-ethyl acetate gradient.

The chosen gradient for the first column provided a better separation of perezone from impurities. From the TLC analysis, some impurities were still present. For the second eluent gradient, the separation failed, perezone was in the 8 first fractions, and more compounds were revealed in the TLC plates.

The amount remaining from hexane extract after passing it through the mini chromatographic column was not enough for further analysis. The total residue from dichloromethane extract weighed 0.803 g.

4.4 Structural Identification of perezone

In order to confirm the presence of perezone in the extracts from *Perezia multiflora's* root, another analysis was made. UPLC-MS, UV-Vis, and voltammetry analysis were made to perezone crystallized and dry DCM extract to compare both.

UPLC-MS analysis was made with the technique ElectroSpray Ionization-Mass Spectrometry (ESI-MS). Negative ESI was chosen because perezone is an acidic compound and tends to form anions in solution. The results obtained with perezone crystallized mass spectrum shows a peak at 247.2029 m/z (Figure 4.8) and the chromatogram shows a retention time of 6.37 min for this mass. The m/z 247.2029 corresponding to the chemical formula of the anionic form of perezone ($C_{15}H_{19}O_3$).

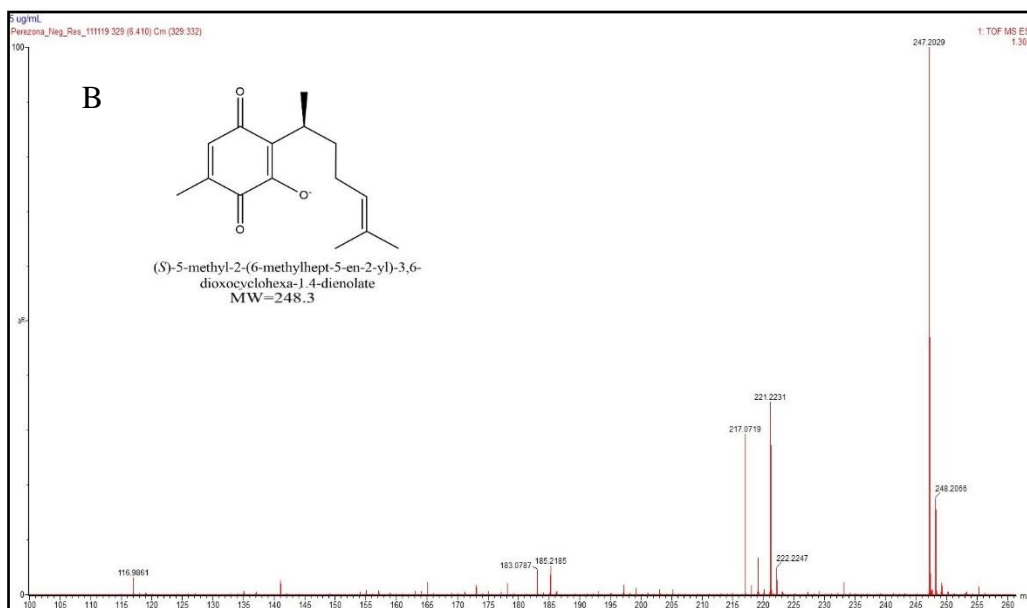
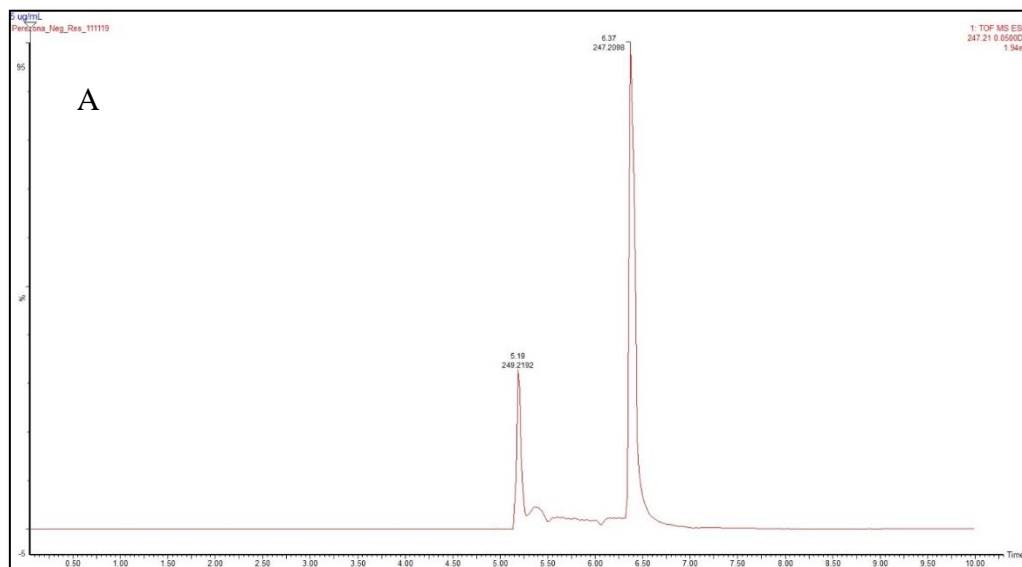


Figure 4.8 Analysis of the perezone crystallized by UPLC-MS. Compound is identify with A) retention time of (RT) = 6.37 min and B) $m/z = 247$.

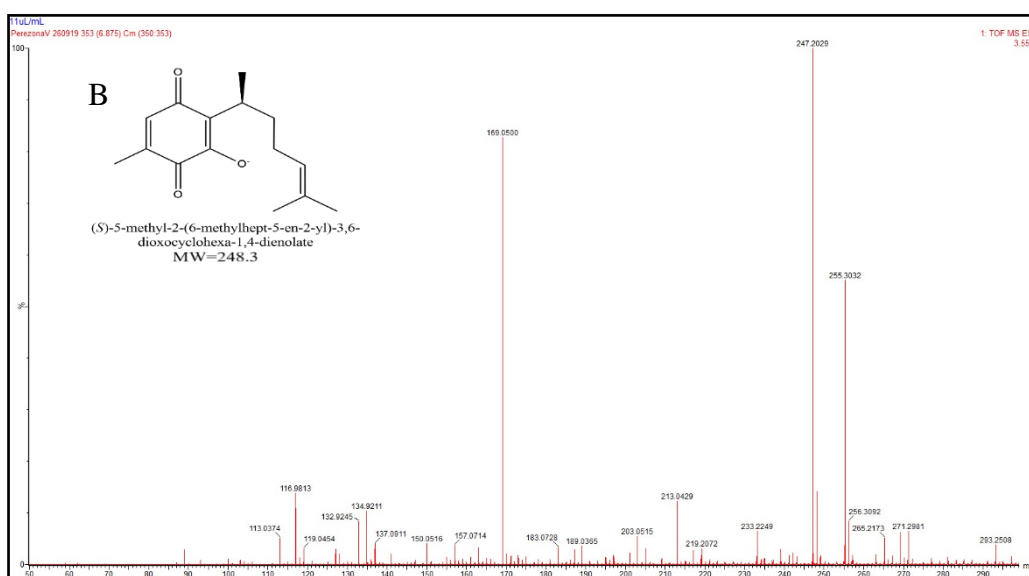
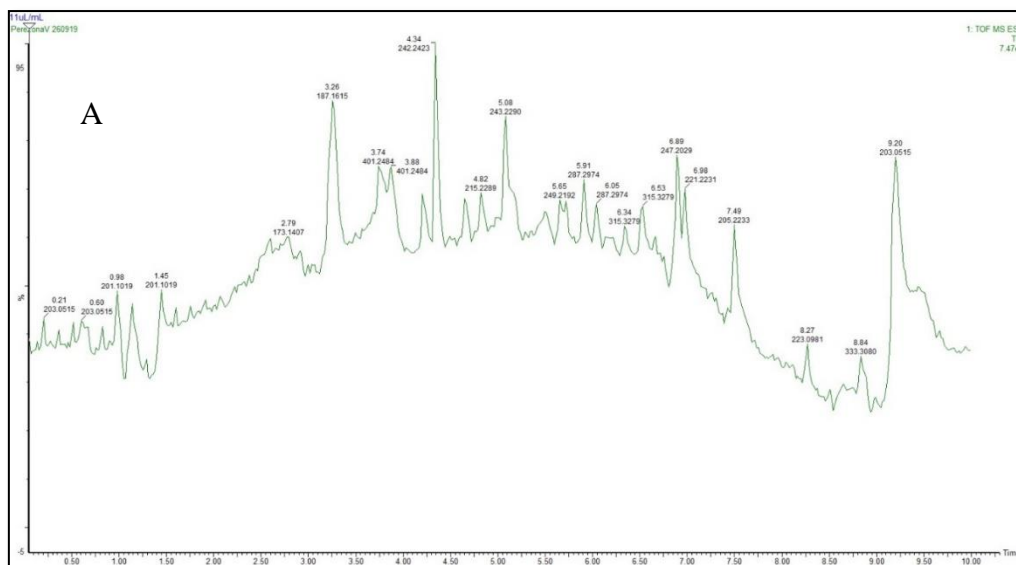


Figure 4.9 Analysis of the dichloromethane extracts of the *P. Multiflora* roots by UPLC-MS. Compound identified with A) retention time of (RT) = 6.89 min and B) $m/z = 247$.

On the other hand, for the mass spectrum of dry dichloromethane extract (Figure 4.9 and Figure 4.8) shows a peak at 247.2029 m/z , which is precisely the mass obtained for perezone crystallized; and the chromatogram shows a retention time of 6.89 min which is close to perezone crystallized.

As we can see in the first chromatogram, the dichloromethane extract shows several peaks indicating the presence of many impurities. Therefore, the extract was filtrated to carry out another chromatogram and seeing a cleaner spectrum (Figure 4.10).

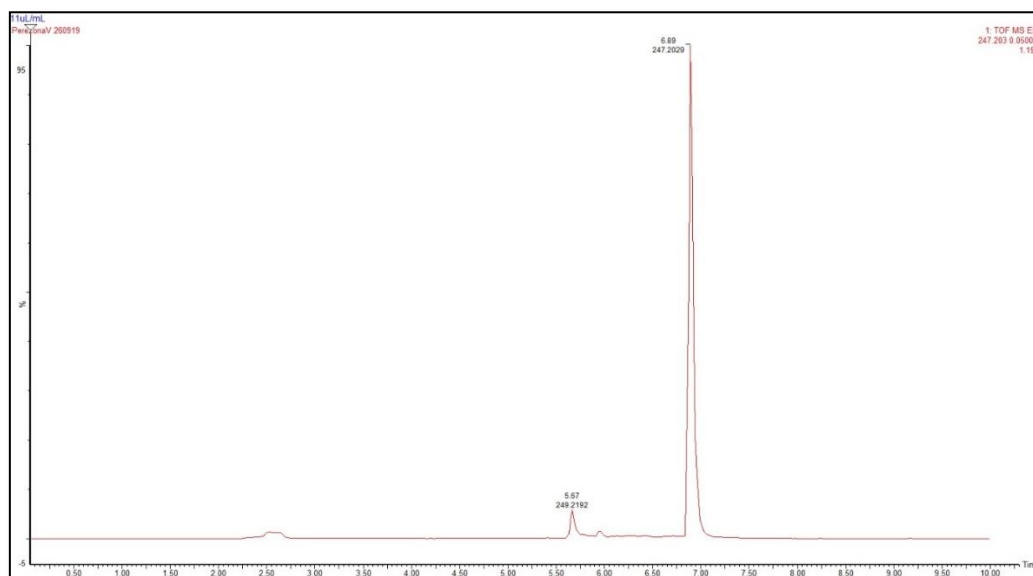


Figure 4.10 Analysis of the dichloromethane extracts filtrated through chromatogram of the *P. Multiflora* roots by UPLC-MS. Compound identify with a retention time of (RT) = 6.89 min.

UV-Vis analysis was made on dry dichloromethane extract and perezone crystallized (Figure 4.11) in order to ensure the presence of perezone in the extract. Perezone crystallized shows two major absorptions peaks at 205 nm and 260 nm; and another small absorption at 410 nm. The UV-Vis absorption spectrum from dry dichloromethane extract agrees with the spectrum from perezone crystallized, with two maxima peaks at 245 nm and 285 nm, but we can observe the peak at 670 nm. Those small differences between both spectrums could be due to a possible anionic form of perezone in the dry dichloromethane extract and the presence of impurities. The anionic form of perezone, characterized with a change in color from yellow to reddish-orange color, could result in a large bathochromic shift and also produce a hyperchromic effect.⁴ The peaks at the region from 205 nm and 285 nm, could be due to π - π^* transition at the quinone ring. The low peak at 410 nm in the case of perezone crystallized and the dry extract peak at observing the peak at 670 nm that could correspond to the n - π^* transition of the quinone carbonyl groups. It is characteristic of the color of perezone in its standard and anionic form respectively, and gives information about the delocalization system of the molecule.

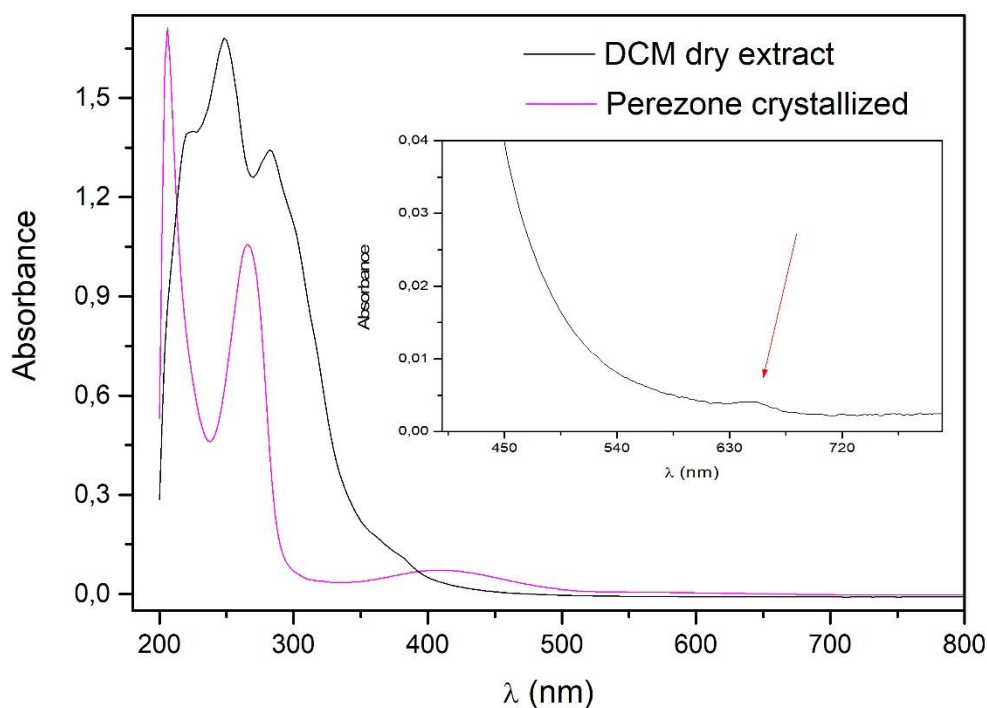


Figure 4.11 UV-Vis spectra in ethanol for perezone crystallized and dry dichloromethane extract from *Perezia Multiflora*.

The analysis and comparison of the oxidation-reduction chemistry between Perezone crystallized, and dichloromethane extract was realized with cyclic voltammetry. The rate was at 50 mV/s. Lithium perchlorate (LiClO_4) was used as the supporting electrolyte at a concentration 0.2M, perezone, and dichloromethane extract at concentration 2mM in DMSO for each experiment. Also, the ferrocene/ferrocenium (Fc/Fc^+) redox couple was used as the internal reference.

The cyclic voltammograms (Figure 4.12) show for Perezone in an aprotic medium three reduction peaks of -1.4V (IIIc), -1.29 V (IIc) y -0.75V(Ic). The first signal IIIc indicates the electronic transfer characteristic of a reversible redox pair with IIIa. The second signal Ic does not form part of the reversible system with a smaller current signal for Ia. Comparing the results with the literature, the third peak at IIc and IIa should be due to protonation of the semiquinone and the rapid reduction of the protonated semiquinone.

For the dichloromethane extract, the voltammogram shows similar behavior to the perezone in negative potential with three reduction peaks but increased peak separation. These three peaks appear at -1.17V (IIIc), -0.89 V (IIc) y -0.67V(Ic). The first peak IIIc appears as a reversible electronic transfer pair with the peak IIIa. Also there the two peaks observed from perezone crystallized disappeared at

DCM extract voltammogram. This should be for degradation of the perezone extracted and also for the impurities present on the sample as the TLC analysis and chromatogram showed it.

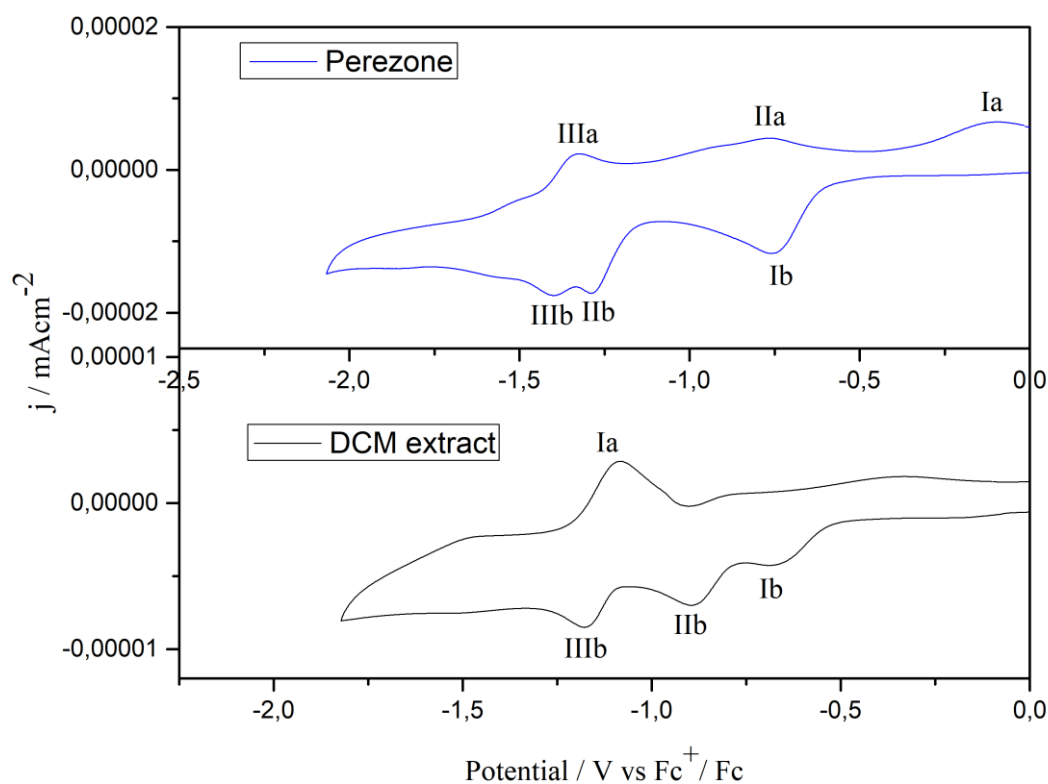


Figure 4.12 Cyclic voltammogram (50 Mv/s) of 2mM perezone crystallized and 2 mM dry dichloromethane extract from *Perezia multiflora*'s roots dissolved in DMSO.

4.5 Synthesis and structural identification for nickel and cobalt-perezone complexes

Cobalt ion generally forms compounds with its oxidation states +2 and +3; the last can be found just in coordinated compounds.⁴⁰ Wicklund et al. reported studies on cobalt catechol complexes and realize that they tend to undergo two one-electron oxidation, and the signals at UV-Vis spectrum for that complexes appeared around 512 nm and 360 nm, in which experiments cobalt ion is coordinated to two orto quinones.⁴¹

The UV-Vis analysis for cobalt-perezone (Figure 4.13) complex was carry out using variation in concentrations of perezone extracted from *Perezia multiflora*'s roots and cobalt salt in ethanol as solvent with total volume of 10 mL for each measurement. In order to find the number of molecules of perezone that are bind to cobalt and nickel metal. The $\text{CoCl}_2 \cdot (\text{H}_2\text{O})_6$ in ethanol yields a violet solution, and when this is mixed with the perezone solution, the solution changed to a kind of lavender

color. The spectrum appears in the interval between 300 nm to 800 nm. Bands at 517 nm and 656 nm can be observed, which inform about the coordination of the metal ions.

We can observe an important change in the form in the second band, it has a bathochromic shift, and the band peak appears at 663 nm.

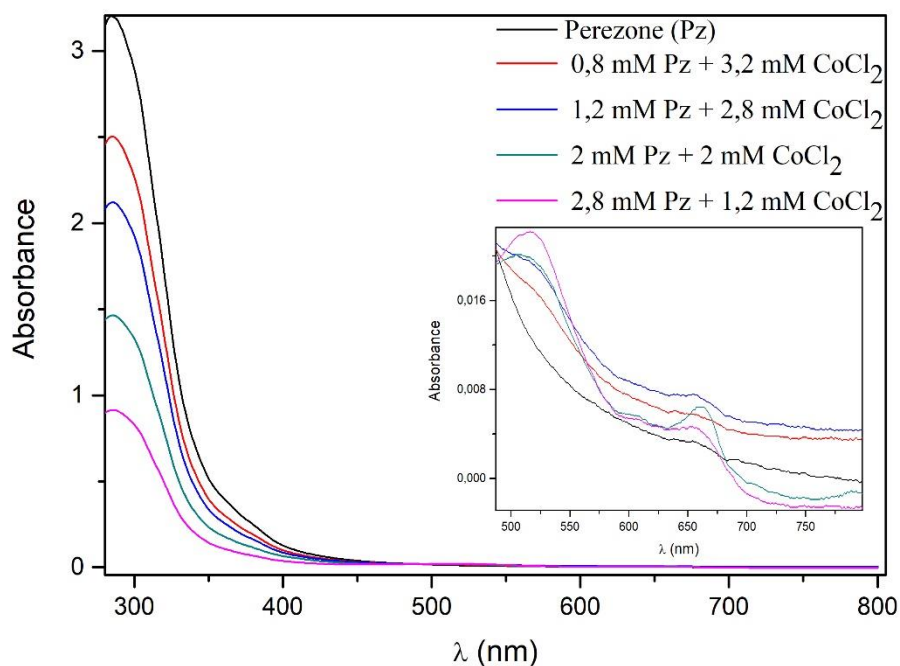


*Figure 4.13 UV-Vis spectra of perezone extracted from *Perezia Multiflora*'s roots and coordination of perezone with $\text{CoCl}_2 \cdot (\text{H}_2\text{O})_6$ at different concentrations in ethanol solvent. All spectrums are carry on with ethanol solvent at a total volume of 10 mL*

For the second analysis, $\text{NiCl}_2 \cdot (\text{H}_2\text{O})_6$ appeared as a green solution in ethanol and turned green yellowish when mixed with the perezone solution. For the nickel-perezone complex, we can observe (Figure 4.14) broadband that shows two peaks at 679 nm and 716 nm. There can be observed that the band for 2:1 perezone/nickel salt has the bigger absorbance indicating the number of perezone that is actually coordinated to cobalt ion.

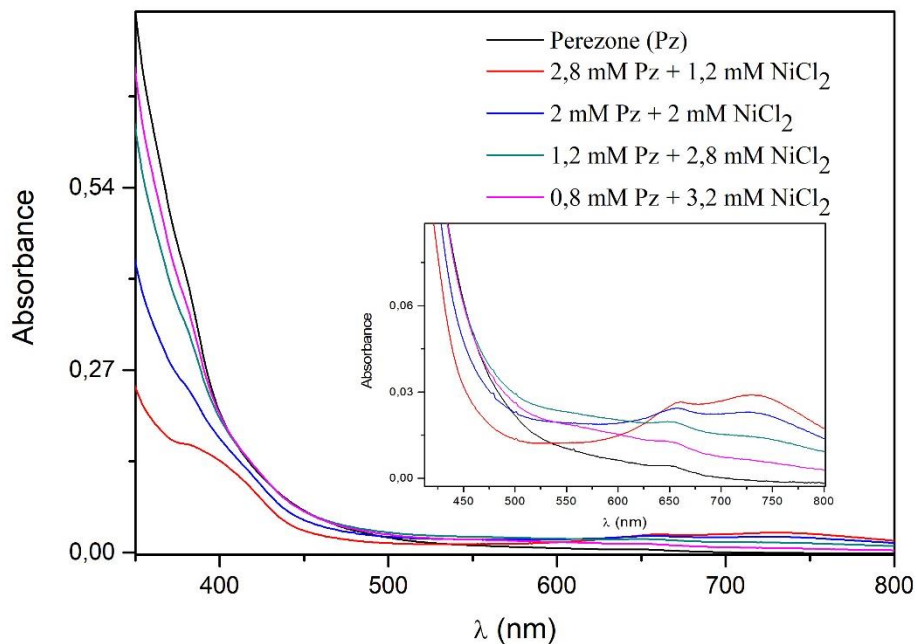


Figure 4.14 UV-Vis spectra of perezone extracted from *Perezia Multiflora* and coordination of perezone with $\text{NiCl}_2 \cdot (\text{H}_2\text{O})_6$ at different concentrations. All spectrums are carry on with ethanol solvent at a total volume of 10 mL

Therefore, the geometries that could be expected for those complexes are octahedral geometry for nickel-perezone complex, and tetrahedral geometry for cobalt-perezone complex (Figure 4.155). The data obtained of magnetic susceptibility and the signals from EPR spectra for both complexes indicate also the proposed geometries. However, more studies must be realized to determine them.

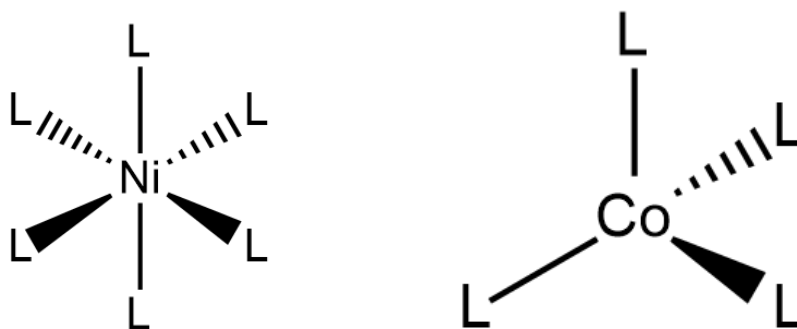


Figure 4.155 Geometries expected for nickel and cobalt-perezone complexes.

4.6 EPR spectroscopy for cobalt and nickel-perezone complexes

One of the main objectives was to determine the magnetic properties of nickel and cobalt-perezone complexes. The experiment for EPR analysis was done for nickel and cobalt- perezone complexes at

different temperatures. As expected, the g -value for organic radical in this case, perezone (Pz), is near to the g value for a free electron. The case of nickel that belongs to the group of transition metal ions with $S = 1$ ground states; such signals are not observable (EPR silent) as they would appear at frequencies beyond the range of conventional EPR spectrometers (high fields and frequencies). However, for the nickel compound studied, we can see the signal in the spectra at the conventional range.

Figure 4.16 and 4.16 shows the dependence of the signal intensity with the temperature; it is notable for both samples and also the difference between powder complex analysis and in water solution. The signal, shapes have an amplitude that decreases at room temperature. We can see an axial symmetry in Ni-3Pz (Figure 4.17) at room temperature and a cubic symmetry at 10K. While for Ni-2Pz (Figure 4.16), the local symmetry also change, there is a axial symmetry at 10K and rhombic at room temperature for water solution; and there is axial symmetry for the complex at room temperature in powder sample.

The hyperfine coupling constant that is found in the distance between peaks in the spectrum indicates the extent of delocalization of unpaired electrons over the molecule.

In Figure 4.16 there is observable the hyperfine interaction for nickel -perezone complex. This is due to the presence of nuclear spins in water solution at room temperature and at 10K for nickel-2perezone, and in Figure 4.17 for nickel-3 perezone, this hyperfine interaction appears with a smaller amplitude.

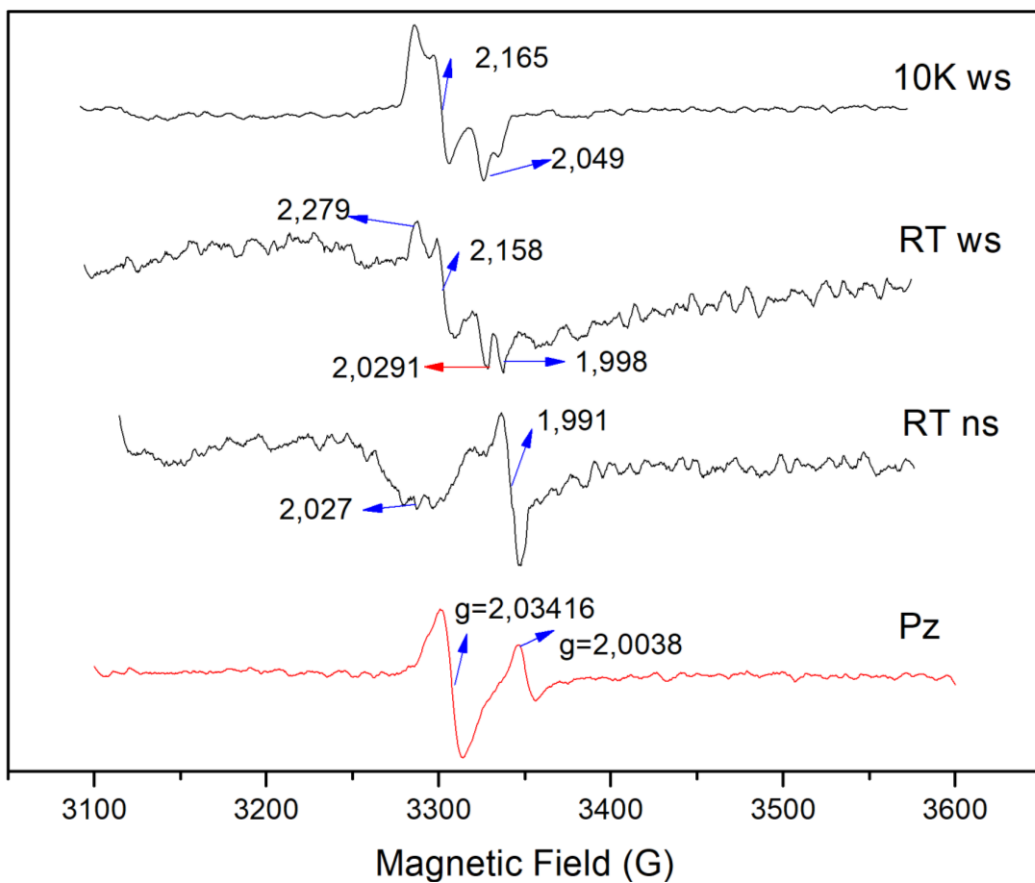


Figure 4.16 EPR spectroscopy of powder (ns) and water solution (ws) of nickel-2perezone complexes at 273K and 10K.

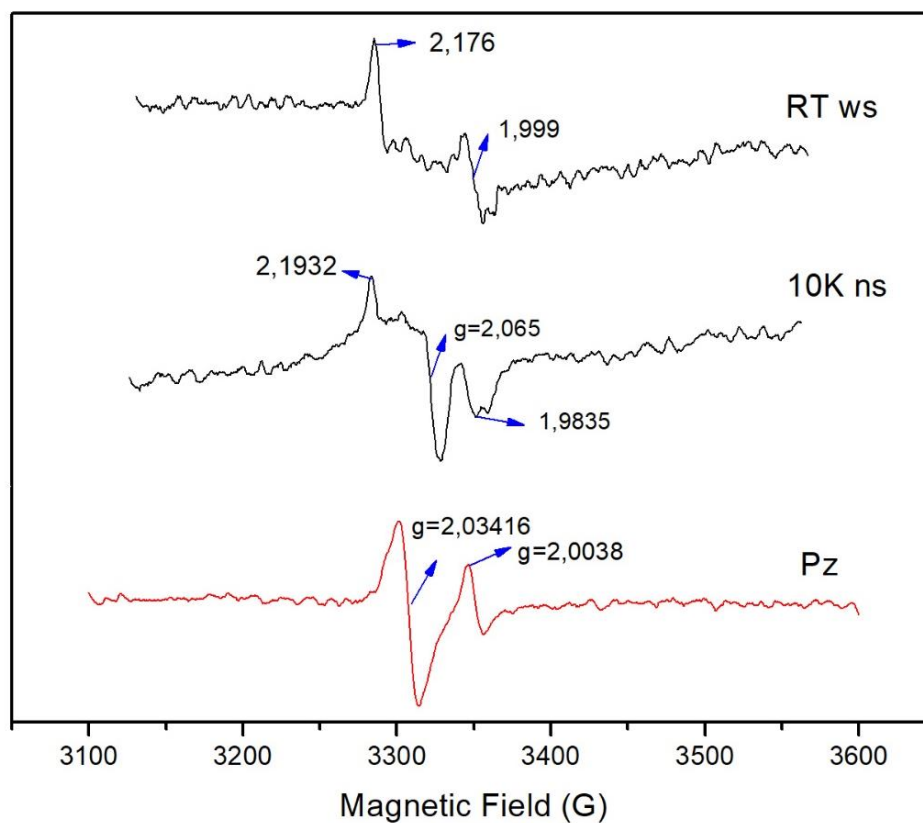


Figure 4.17 EPR spectroscopy of powder (ns) and water solution (ws) of nickel-3perezone complexes at 273K and 10K

For the case of cobalt that belongs to the group of transition metal ions with $S = 3/2$ ground state, contrary to nickel ion, their signals are observable at low frequencies of conventional EPR spectrometers. Figure 4.17 shows the EPR spectrum for the cobalt-perezone complex in powder form; there is an isotropic pattern at 10K temperature. The lack of hyperfine coupling could be due to the electron transfer reaction between perezone and cobalt ion is weak.³¹

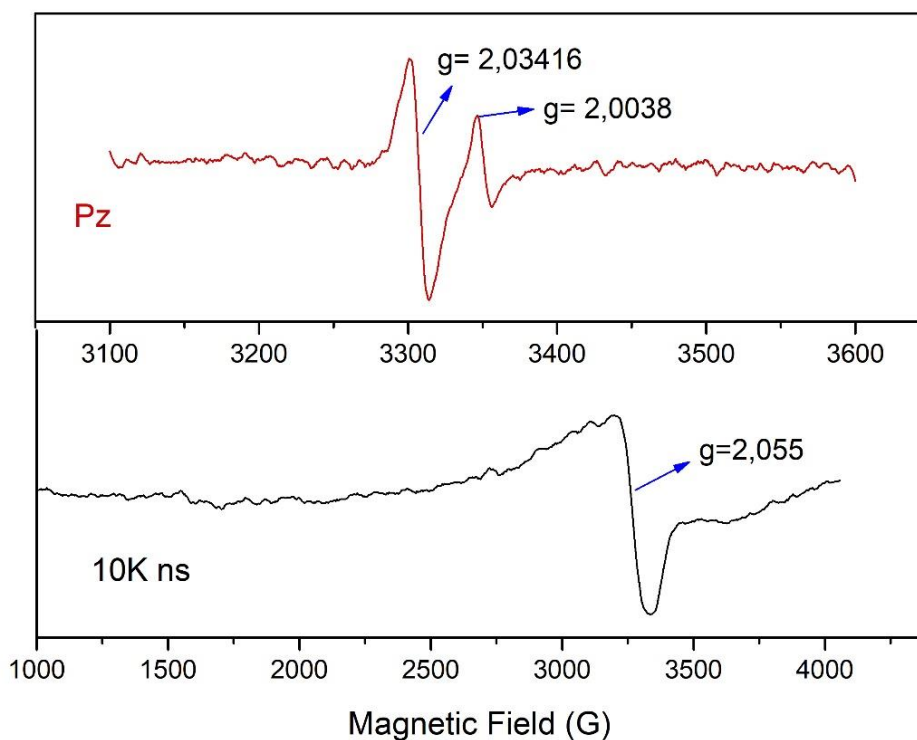


Figure 4.18 EPR spectroscopy of powder (Pz) and ethanolic solution (ns) of cobalt-3perezone complex at 10K

4.7 Magnetism for nickel and cobalt complexes

In order to know the magnetic properties, it was used the Curie-Weiss law equation to plot and identify the kind of material we had for cobalt and nickel- perezone complexes. Magnetic susceptibility measurements made over a range of temperatures between 0-300K, allowed to identify the magnetic properties of the cobalt and nickel complexes.

Cobalt(II) ion, $3d^7$ configuration with three unpaired electrons. This ion is expected to have three unpaired electrons in tetrahedral and octahedral geometries.³⁷

For a free cobalt ion:

$$S = 3/2$$

$$L = 3$$

$$\mu_{\text{only spin}} = 2 \sqrt{S(S+1)} = 3.87$$

$$\mu_{\text{Spin-orbit}} = \sqrt{L(L+1)} + 4S(S+1) = 5.20 \text{ B.M}$$

Nickel(II) ion, $3d^8$ configuration with two unpaired electrons. For the case of nickel ions, the tetrahedral geometry uses to have higher magnetic moments than for octahedral.³⁷

For a free nickel ion

$$S=1$$

$$L = 3$$

$$\mu_{\text{only spin}} = 2 \sqrt{S(S+1)} = 2.83$$

$$\mu_{\text{Spin-orbit}} = \sqrt{L(L+1) + 4S(S+1)} = 4.47 \text{ B.M}$$

Figure 4.19. shows a typical temperature scan versus magnetic susceptibility plot and temperature versus an effective magnetic moment for both complexes. This figure shows the resulting characteristic plot that identifies cobalt-perezone and nickel-perezone complexes with Neel temperatures $T_N = 1.79$ and $T_N = 1.99$, respectively. In Figure 4.19. we can see that the value of μ_{eff} at 300K is 3.64 MB for nickel-perezone complex; this is bigger than the expected value for just spin magnetic moment; and is 4.6 MB for cobalt this is bigger value for the just spin magnetic moment. When the temperature decreases, the magnitude of the magnetic moment decreases until it reaches a value of 2.97 BM for Cobalt and 1.69 BM for nickel, those are closed to the value of just spin magnetic moment. This behavior indicates antiferromagnetic interaction in the molecule. Therefore, according to the experimental magnetic moments obtained, for nickel-perezone complexes, it has an octahedral geometry. Furthermore, for the cobalt-perezone complex, it has a tetrahedral geometry.³⁷

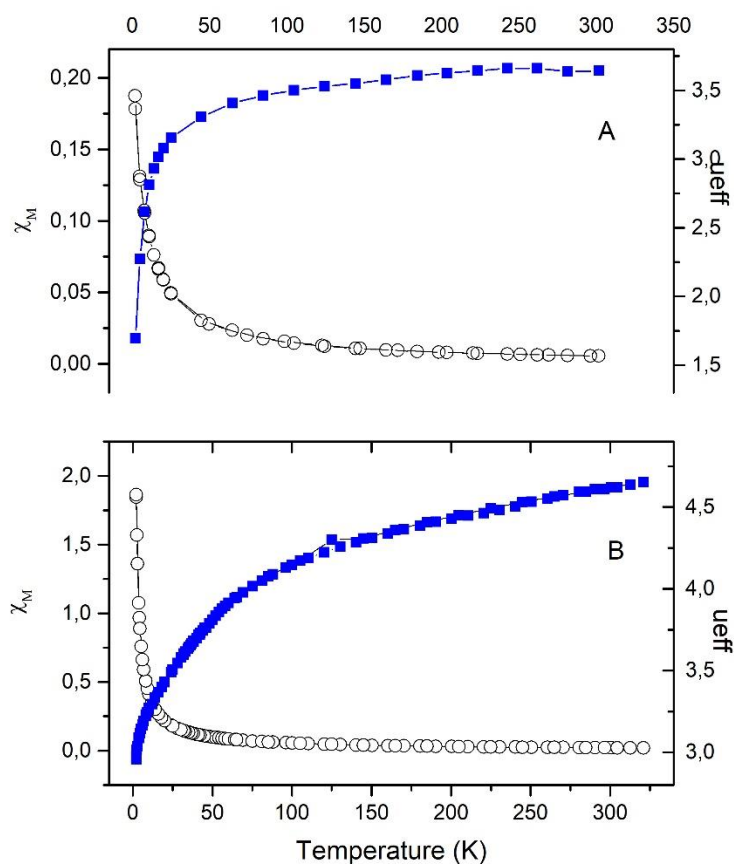


Figure 4.19 Plot magnetic susceptibility (left axis) and effective magnetic moment (right axis) versus temperature for the two complexes. A) Nickel-perezone complex and B) Cobalt-perezone complex

In a large class of materials, there is a linear relationship between magnetization and the magnetic field applied. According to the following equation, when χ is negative, the material is diamagnetic, and when χ is positive, the material is paramagnetic. The value of the slopes is small 0.7938 for cobalt and 0.1487 for nickel complex.

$$M = \chi H$$

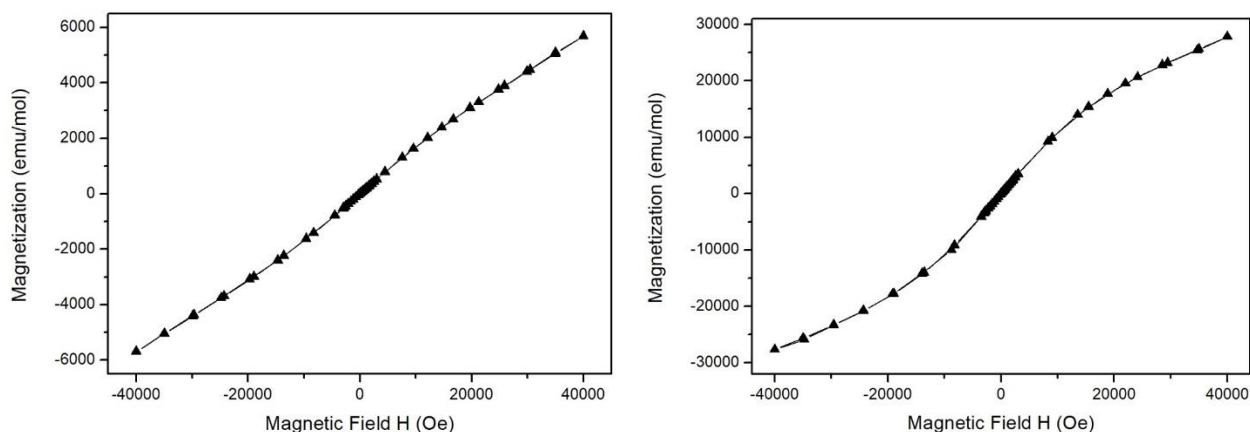


Figure 4.20 Magnetization versus applied field for both compounds nickel-perezone (left) and cobalt-perezone (right).

The plot of inverse susceptibility against temperature and product of magnetic susceptibility by temperature versus temperature provides the images easier to identify the magnetic behavior of both compounds. In Figure 4.21 the characterization of magnetic behavior is more notable for nickel-perezone and cobalt-perezone complexes, as T increase, the values for $\chi_M * T$ indicating the antiferromagnetic behavior.

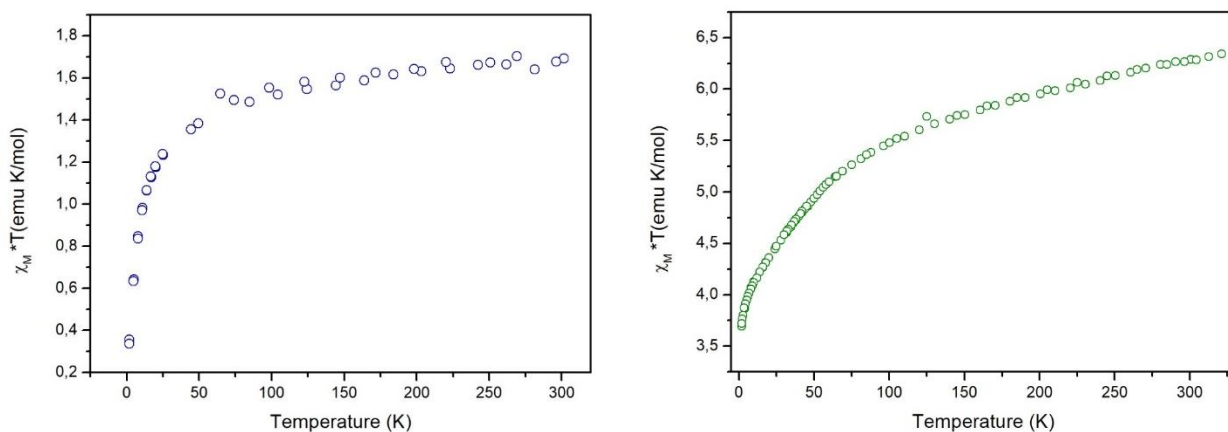


Figure 4.21 The product $\chi_M * T$ for nickel-perezone(left) and cobalt-perezone(right) complexes as a function of temperature.

In Figure 4.22 for nickel and cobalt-perezone complexes, following a straight line above T_N , which extrapolates to a negative value at the temperature, $\Theta = -9.796$ K and $\Theta = -10.394$ K respectively. This small value for Weiss constant indicates a weak molecular field and, therefore, low transition temperature between paramagnetic and antiferromagnetic. In addition, measurement of the slope shows the Curie-Weiss constant, C equal to 1.722 and 6.3572 (moles/emu.K) for Nickel and cobalt complex. From molecular field theory, Θ is a measure of the interaction strength between magnetic moments. The value of this constant is negative and, therefore, the characteristic of antiferromagnetic material.

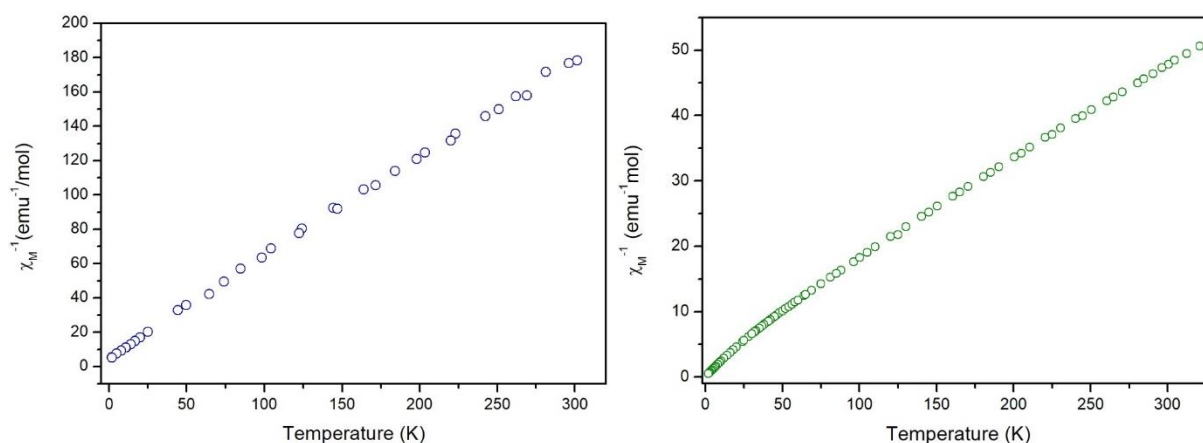


Figure 4.22 Inverse susceptibility versus temperature at a field strength of Gauss applied for nickel-perezone(left) and cobalt-perezone(right) complexes.

4. Conclusion

- From comparing the characteristics of the plant with the literature, the escorzonera plant bought in a market of Tungurahua province is confirmed to correspond to the *Perezia multiflora* species.
- Through chromatographic analysis (TLC), using a standard sample of perezone crystallized, the result showed the presence of perezone in both extracts from escorzonera's roots. Furthermore, it was observed that the extraction with hexane provides fewer impurities for perezone extraction, when is compared with dichloromethane extraction. Provoking more work to isolate and purify perezone from dichloromethane extract, as the column chromatography.
- After the isolation of perezone from dichloromethane extract through column chromatography, we obtained an oily residue similar to the hexane extract but still oily residue. The residue from dichloromethane extract had a yield of 1%, and the extract from hexane yields less than 1% of perezone from Escorzonera (*Perezia multiflora*).
- The presence of perezone was confirmed through UV-VIS spectroscopy, UPLC-MS, and Cyclic voltammetry analysis. Perezone is present in the roots of *Perezia multiflora*. However, more structural analysis should be made on extracts.
- The bands observed in the UV-Vis spectrum for dichloromethane extract was the same as observed with the standard sample of Perezone but with a bathochromic shift. The anionic form of perezone and the presence of impurities could be the reason for the bathochromic shift observed in the UV-Vis spectra.
- The voltammetry analysis for the standard perezone and the extracts showed a third peak that could be explained with the protonation of perezone; this could be due to the no dry DMSO solvent. There was also the lack of two oxidation peaks in the voltammogram that could be due to a degradation of the perezone in the DCM extract or the presence of impurities.
- In order to synthesize the nickel and cobalt complexes, a variation in concentration of perezone and nickel was made. The analysis through the UV-Vis spectrum gives, as a result, the coordination of perezone with cobalt and nickel ions, having 1:1 and 2:1, respectively.

- Although nickel is silent EPR at low frequencies, in EPR measurements, nickel-perezone signals appear as axial and cubic shape. For the case of the cobalt-perezone complex, the signal was isotropic. The magnetism studies showed that the complexes of perezone with cobalt and nickel salts have an antiferromagnetic behavior.
- To date, antiferromagnetic materials are used on devices such as high density memories, and also are used to modify the behavior of ferromagnetic materials.⁴² Also, those compounds have interesting application on magnetic Radom access memories (MRAM)^{43,42} is hoped that further studies should carry on the synthesis and other possible application of the complexes synthetized on this work.

5. Bibliography

- (1) Enríquez, R.; Ortega, J.; Lozoya, X. Active Components in *Perezia* Roots. *J. Ethnopharmacol.* **1980**, *2* (4), 389–393. [https://doi.org/10.1016/S0378-8741\(80\)81018-X](https://doi.org/10.1016/S0378-8741(80)81018-X).
- (2) Zdero, C.; Bohlmann, F.; Solomon, J.; Dominguez, X. A. Further Isocedrene Derivatives and Other Constituents from *Perezia* Species. *Phytochemistry* **1988**, *27* (3), 849–853. [https://doi.org/10.1016/0031-9422\(88\)84105-0](https://doi.org/10.1016/0031-9422(88)84105-0).
- (3) Tamariz-Angeles, C.; Olivera-Gonzales, P.; Santillán-Torres, M. Antimicrobial, Antioxidant and Phytochemical Assessment of Wild Medicinal Plants from Cordillera Blanca (Ancash, Peru). *Bol. Latinoam. y del Caribe Plantas Med. y Aromat.* **2018**, *17* (3), 270–285.
- (4) Gómez-Serrano, G.; Cristiani-Urbina, E.; Villegas-Garrido, T. L. Time-Dependent Perezone Production in Different Culture Systems of *Acourtia Cordata*. *Cent. Eur. J. Biol.* **2012**, *7* (3), 507–518. <https://doi.org/10.2478/s11535-012-0035-2>.
- (5) Lozada, C. M.; Soria-Arteche, O.; Ramírez Apan, T. M.; Nieto-Camacho, A.; Enríquez, R. G.; Izquierdo, T.; Jiménez-Corona, A. Synthesis, Cytotoxic and Antioxidant Evaluations of Amino Derivatives from Perezone. *Bioorganic Med. Chem.* **2012**, *20* (17), 5077–5084. <https://doi.org/10.1016/j.bmc.2012.07.027>.
- (6) Abraham, I.; Joshi, R.; Pardasani, P.; Pardasani, R. T. Recent Advances in 1,4-Benzoquinone Chemistry. *J. Braz. Chem. Soc.* **2011**, *22* (3), 385–421.
- (7) Burgueño-Tapia, E.; Castillo, L.; González-Coloma, A.; Joseph-Nathan, P. Antifeedant and Phytotoxic Activity of the Sesquiterpene P-Benzoquinone Perezone and Some of Its Derivatives. *J. Chem. Ecol.* **2008**, *34* (6), 766–771. <https://doi.org/10.1007/s10886-008-9495-2>.
- (8) Carabez, A.; Sandoval, F. The Action of the Sesquiterpenic Benzoquinone, Perezone, on Electron Transport in Biological Membranes. *Arch. Biochem. Biophys.* **1988**, *260* (1), 293–300.
- (9) Gawali, S. S.; Dalvi, R.; Ah, K.; Rane, S. Thermal, Magnetic and Spectral Studies

- of Metal-Quinone Complexes Part II. Media Effect on Coligation of Aqua Ligands. *J. Therm. Anal. Calorim.* **2004**, 76 (3), 801–812. <https://doi.org/10.1023/B:JTAN.0000032265.45347.3d>.
- (10) Aguilar-Martinez, M.; Macias-Ruvalcaba, N.; Bautista-Martinez, J.; Gomez, M.; Gonzalez, F.; Gonzalez, I. Review: Hydrogen Bond and Protonation as Modifying Factors of the Quinone Reactivity. *Curr. Org. Chem.* **2005**, 8 (17), 1721–1738. <https://doi.org/10.2174/1385272043369548>.
- (11) Prince, R. C.; Lloyd-Williams, P.; Malcolm Bruce, J.; Leslie Dutton, P. [8] Voltammetric Measurements of Quinones. *Methods Enzymol.* **1986**, 125 (C), 109–119. [https://doi.org/10.1016/S0076-6879\(86\)25010-7](https://doi.org/10.1016/S0076-6879(86)25010-7).
- (12) Brunmark, A.; Cadenas, E. Redox and Addition Chemistry of Quinoid Compounds and Its Biological Implications. *Free Radic. Biol. Med.* **1989**, 7, 435–477.
- (13) Song, Y.; Buettner, G. R. Thermodynamic and Kinetic Considerations for the Reaction of Semiquinone Radicals to Form Superoxide and Hydrogen Peroxide. *Free Radic. Biol. Med.* **2010**, 49 (6), 919–962. <https://doi.org/10.1016/j.freeradbiomed.2010.05.009>.
- (14) Monks, T.; Hanzlink, R.; Cohen, G. M.; Ross, V. D. Contemporary Issues in Toxicology. Quinone Chemistry and Toxicity. *Biochemistry* **1992**, 16 (2), 2–16. <https://doi.org/0041408X>.
- (15) Guin, P. S.; Das, S.; Mandal, P. C. Electrochemical Reduction of Quinones in Different Media: A Review. *Int. J. Electrochem.* **2011**, 2011, 1–22. <https://doi.org/10.4061/2011/816202>.
- (16) González, I.; Frontana, C.; Gómez, M.; Aguilar, M.; Bautista, J. A.; Macías, N. A.; Salas, M.; Astudillo, P. D.; González, F. J. Modifying the Reactivity of Reduced Intermediates of Quinones by Structural Changes and Intra and Intermolecular Hydrogen Bonding. *ECS Trans.* **2007**, 3 (29), 25–36. <https://doi.org/10.1149/1.2753288>.
- (17) Vigalok, A.; Milstein, D. Advances in Metal Chemistry of Quinonoid Compounds: New Types of Interactions between Metals and Aromatics. *Acc.*

Chem. Res. **2001**, *34* (10), 798–807.

- (18) Abreu, P. A.; Wilke, D. V.; Araujo, A. J.; Marinho-Filho, J. D. B.; Ferreira, E. G.; Ribeiro, C. M. R.; Pinheiro, L. S.; Amorim, J. W.; Valverde, A. L.; Epifanio, R. A.; et al. Perezone, from the Gorgonian Pseudopterogorgia Rigida, Induces Oxidative Stress in Human Leukemia Cells. *Brazilian J. Pharmacogn.* **2015**, *25* (6), 634–640. <https://doi.org/10.1016/j.bjp.2015.07.020>.
- (19) Nagamura, N.; Taniki, R.; Kitada, Y.; Masuda, A.; Kobayashi, H.; Oka, N.; Honma, I. Electronic States of Quinones for Organic Energy Devices: The Effect of Molecular Structure on Electrochemical Characteristics. *ACS Appl. Energy Mater.* **2018**, *1* (7), 3084–3092. <https://doi.org/10.1021/acsaem.7b00156>.
- (20) Widholm, J M, T. N. (Managing E. H. L. J. M. W.; Widholm, J. M. *Biotechnology in Agriculture and Forestry*; 2005; Vol. 62. https://doi.org/10.1007/978-3-642-13440-1_3.
- (21) Vega Portalatino, E.; López Medina, E. Concentración Mínima Inhibitoria Del Extracto Hidroalcohólico de Tallos y Hojas de Baccharis Genistelloides, Perezia Multiflora, Senecio Sublutescens YJungia Paniculata Del Parque Nacional Huascarán (Perú) Frente a Cepas Bacterianas de Interés Clínico. *Rev. REBIOLEST* **2013**, *1* (2), 43–49.
- (22) Días, L. Guía de Plantas Alto Pita. *FONAG* **2018**, 1–240.
- (23) Joseph-Nathan, P.; Hidalgo, J.; Abramo-Bruno, D. A New Coumarin from Perezia Multiflora. *Phytochemistry* **1978**, *17* (3), 583–584. [https://doi.org/10.1016/S0031-9422\(00\)89384-X](https://doi.org/10.1016/S0031-9422(00)89384-X).
- (24) Roura-Pérez, G.; Quiróz, B.; Aguilar-Martínez, M.; Frontana, C.; Solano, A.; González, I.; Bautista-Martínez, J. A.; Jiménez-Barbero, J.; Cuevas, G. Remote Position Substituents as Modulators of Conformational and Reactive Properties of Quinones. Relevance of the π/π Intramolecular Interaction. *J. Org. Chem.* **2007**, *72* (6), 1883–1894. <https://doi.org/10.1021/jo061576v>.
- (25) Soriano-garcia, B. Y. M.; Toscano, R. A.; Montoya-Vega, F.; Flores-Valderde, E.; Lopez-Celis, I. Structure of 2-(1,5-Dimethyl-4-Hexenyl)-3-Hydroxy-5-Methyl-

- 1,4-Benzoquinone (Perezona), a Sesquiterpene. **1986**, No. 1978, 30327–30329.
- (26) Urbán Martínez, G. A.; Aceves Pastrana, P. E. Leopoldo Río de La Loza En La Institucionalización de La Química Mexicana. *Rev. la Soc. Química México* **2001**, *45* (1), 35–39.
- (27) Andrea, V.; Mart, A.; Mendoza, P.; Saavedra-leos, Z.; Cruz-olivares, J.; Serrano, J. N.; Mart, J.; Ruvalcaba, M. Green Approach Extraction of Perezona from A Comparison of Four Activating Modes and Supercritical Carbon Dioxide.
- (28) Escobedo-González, R. G.; Bahena, L.; Arias Tellez, J. L.; Hinojosa Torres, J.; Ruvalcaba, R. M.; Aceves-Hernández, J. M. Characterization and Comparison of Perezona with Some Analogues. Experimental and Theoretical Study. *J. Mol. Struct.* **2015**, *1097*, 98–105. <https://doi.org/10.1016/j.molstruc.2015.05.016>.
- (29) Company, S. P.; Pierpont, G.; Buchanan, M. Transition Metal Complexes of O-Benzoquinone, o-Semiquinone, and Caathecolate Ligands. *Coord. Chem. Rev.* **1981**, *38* (198 1), 45–87.
- (30) Kaim, W.; Schwederski, B. Non-Innocent Ligands in Bioinorganic Chemistry — An Overview. **2010**, *254*, 1580–1588. <https://doi.org/10.1016/j.ccr.2010.01.009>.
- (31) Boles, K. A. *Electrochemistry of Tris(Tetrachlorocatecholate) Complexes of Manganese, Iron, and Cobalt*; Colorado, 2014.
- (32) Hirao, T. Conjugated Systems Composed of Transition Metals and Redox-Active π -Conjugated Ligands. *Coord. Chem. Rev.* **2002**, *226* (1–2), 81–91. [https://doi.org/10.1016/S0010-8545\(01\)00436-2](https://doi.org/10.1016/S0010-8545(01)00436-2).
- (33) Weil, J.; Bolton, J. *Electron Paramagnetic Resonance. Elementary Theory and Practical Applications*, Second Edi.; Wiley Interscience: Canada, 2007.
- (34) Brustolon, M.; Giamello, E. *Electron Paramagnetic Resonance. A Practitioner's Toolkit*; Wiley, 2009.
- (35) Benelli, C.; Gatteschi, D. *Introduction to Molecular Magnetism. From Transition Metals to Lanthanides*; Wiley-VCH: Germany, 2015.

- (36) (Studies in Inorganic Chemistry 16) F.E. Mabbs and D. Collison (Eds.)-Electron Paramagnetic Resonance of d Transition Metal Compounds-Elsevier Science (1992).
- (37) Earnshaw, A. *Introduction to Magneto Chemistry*; Alden and Mowbray Ltd.: London, 1968.
- (38) Getzlaff, M. *Fundamentals of Magnetism*; Springer: Germany, 2008.
- (39) Martínez, A. L.; Madariaga-Mazón, A.; Rivero-Cruz, I.; Bye, R.; Mata, R. Antidiabetic and Antihyperalgesic Effects of a Decoction and Compounds from *Acourtia Thurberi*. *Planta Med.* **2017**, *83* (6), 534–544. <https://doi.org/10.1055/s-0042-119652>.
- (40) Yildiz, Y. *General Aspects of the Cobalt Chemistry General Aspects of the Cobalt Chemistry*; Maaz, K., Ed.; Intech: Croatia, 2017. <https://doi.org/10.5772/intechopen.71089>.
- (41) Wicklund, P.; Lynn, B.; Dennis, B. Preparation and Properties of a Stable Semiquinone Complex. *Inorg. Chem.* **1976**, *15* (8), 1996–1997.
- (42) Mandziak, A.; D. Soria, G.; Prieto, J. E.; Prieto, P.; Granados-Miralles, C.; Quesada, A.; Foerster, M.; Aballe, L.; de la Figuera, J. Tuning the Néel Temperature in an Antiferromagnet: The Case of $\text{Ni}_x\text{Co}_{1-x}\text{O}$ Microstructures. *Sci. Rep.* **2019**, *9* (1), 1–8. <https://doi.org/10.1038/s41598-019-49642-8>.
- (43) Rinaldi-Montes, N.; Gorria, P.; Martínez-Blanco, D.; Fuertes, A. B.; Puente-Orench, I.; Olivi, L.; Blanco, J. A. Size Effects on the Néel Temperature of Antiferromagnetic NiO Nanoparticles. *AIP Adv.* **2016**, *6* (5). <https://doi.org/10.1063/1.4943062>.